Supported in part by
U.S. DEPARTMENT OF ENERGY

Highlights from STAR beam energy scan II program

Alexey Aparin for the STAR collaboration
Joint Institute for Nuclear Research

Beam Energy Scan to map the QCD phase diagram

Two phases of Beam Energy Scan:
Phase I: 7.7 – 39 GeV 2010 – 2014
First glance at low energy region, rather low statistics

Phase II: 3 – 54.4 GeV 2017 – 2021
Precise measurements at low energies, large statistics

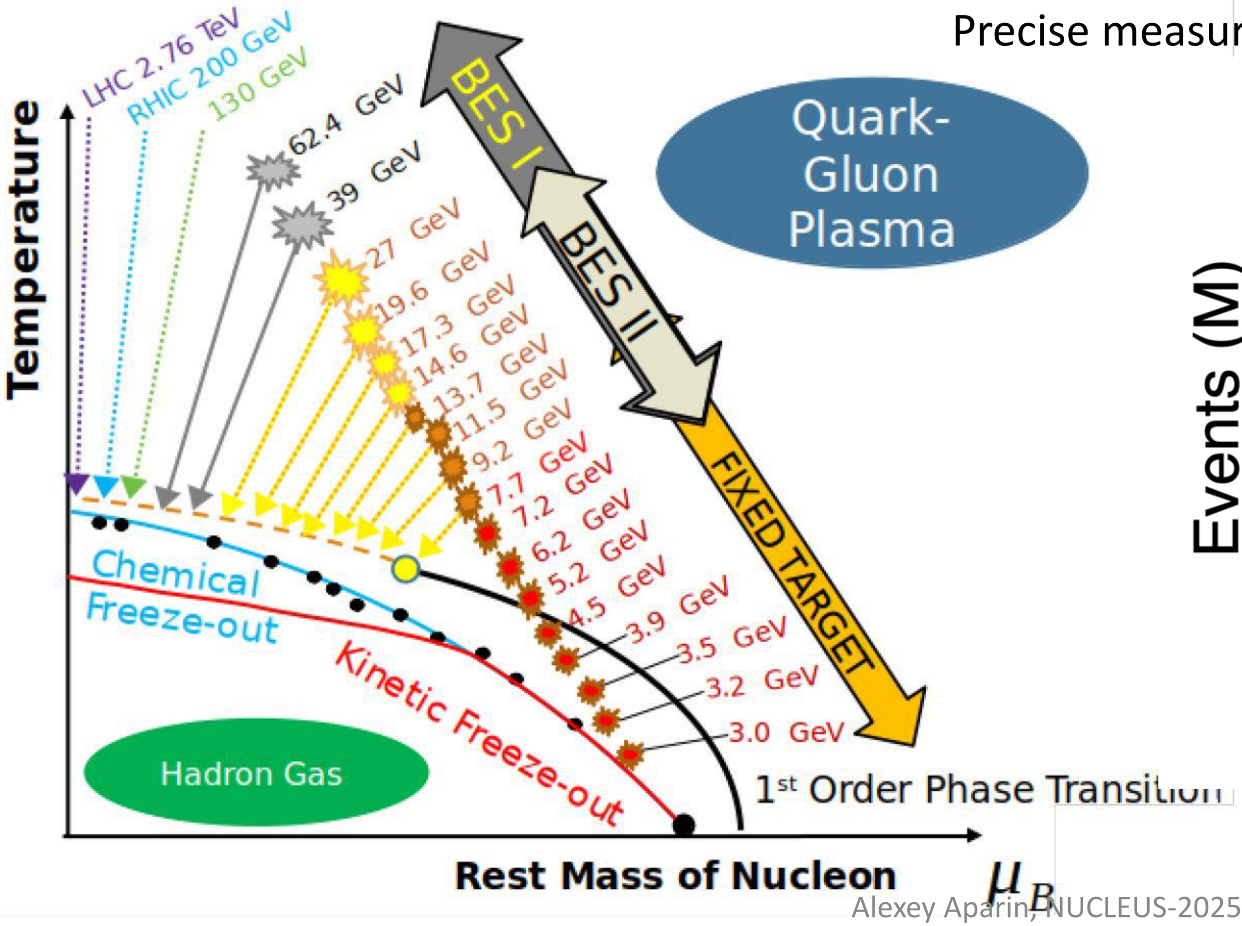

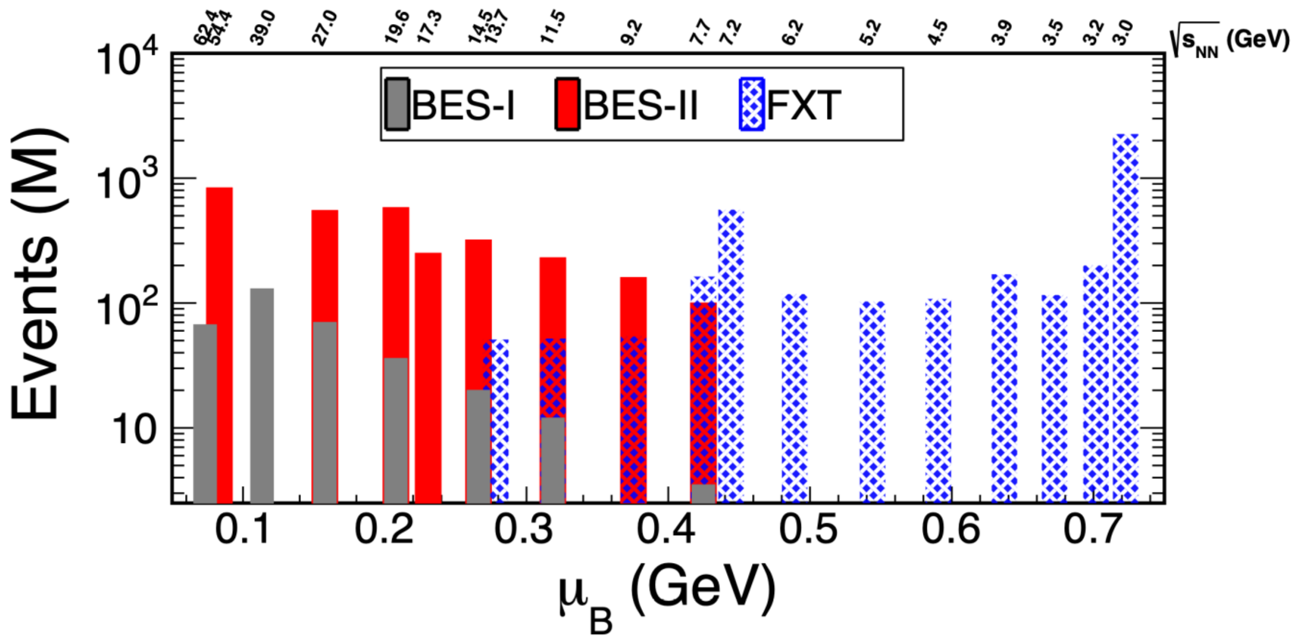

STAR detector

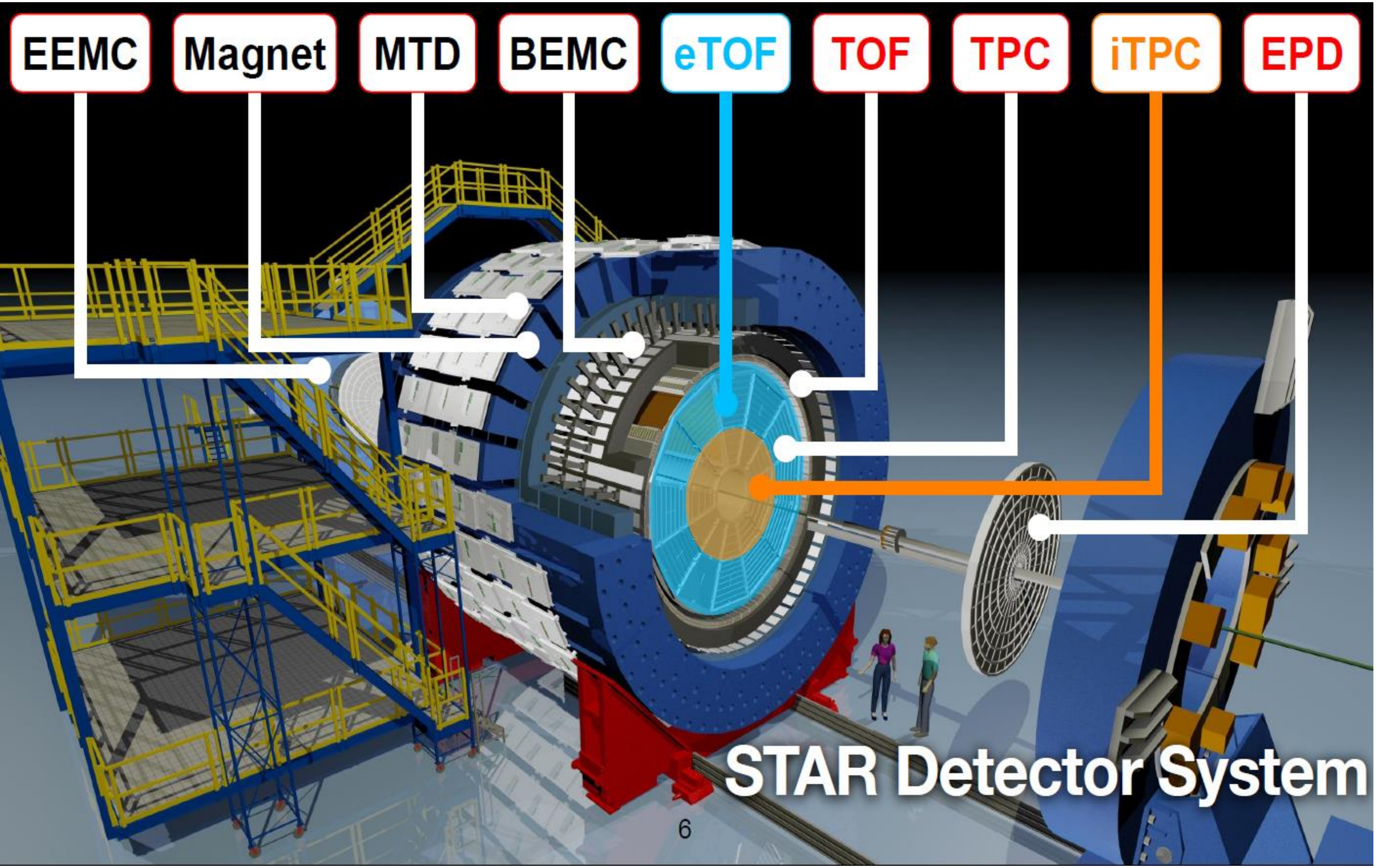

- **Tracking and PID (full 2π)**
  TPC: |η| < 1
  iTPC (2019+): |η| < 1.5
  TOF: |η| < 1
  eTOF (2019+): -1.6 < η < -1
  BEMC: |η| < 1
  EEMC: 1 < η < 2
  HFT (2014-2016): |η| < 1
  MTD (2014+): |η| < 0.5 (partial azimuthal coverage)

- **MB trigger and event plane reconstruction**
  BBC (before 2018): 3.3 < |η| < 5
  EPD (2018+): 2.1 < |η| < 5.1
  VPD: 4.2 < |η| < 5
  ZDC: 6.5 < |η| < 7.5

Directed flow at low energies

$$E\frac{d^3N}{dp^3}=\frac{1}{2\pi}\frac{d^2N}{p_t dp_t dy}\left(1+\sum_{n=1}^{\infty}2v_n\cos\left[n(\varphi-\Psi_r)\right]\right)$$

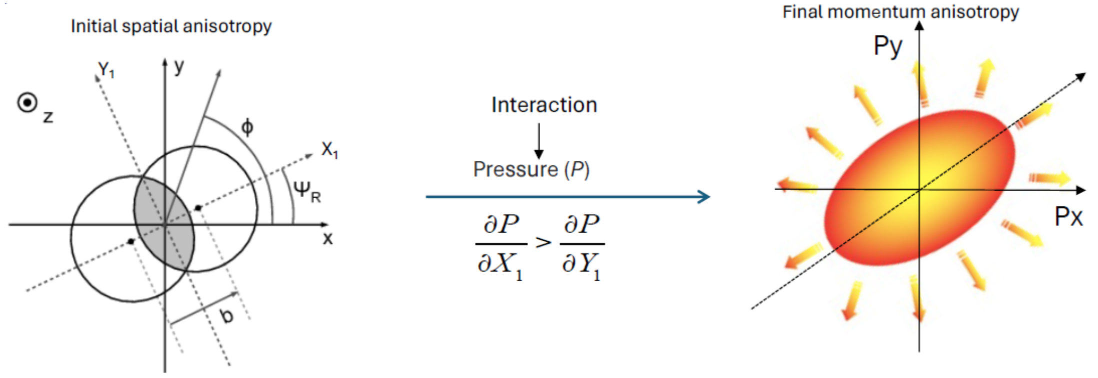

Flow is formed at very early stages of collision – sensitive to initial eccentricity, EoS and shadowing from the spectators at low energies

ϕ meson follows the trend of proton and **Λ**

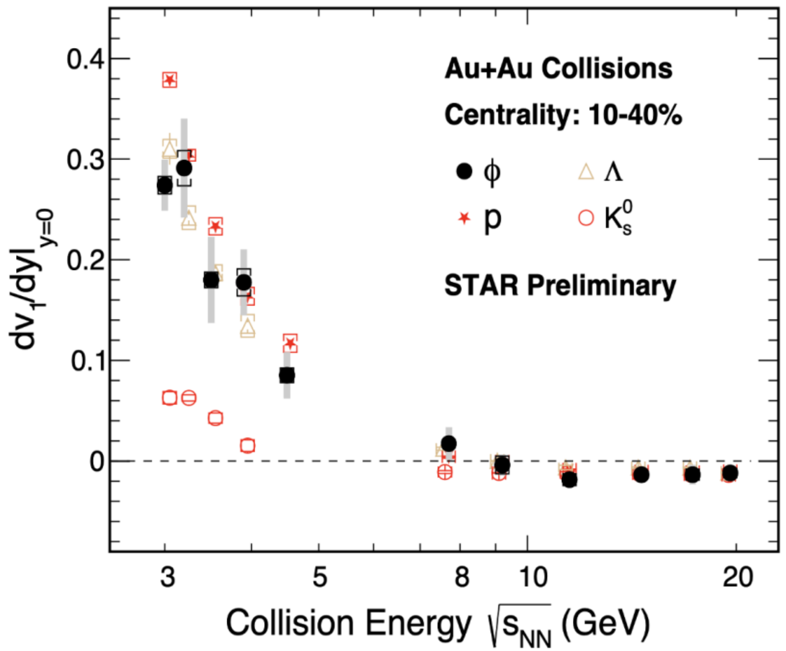

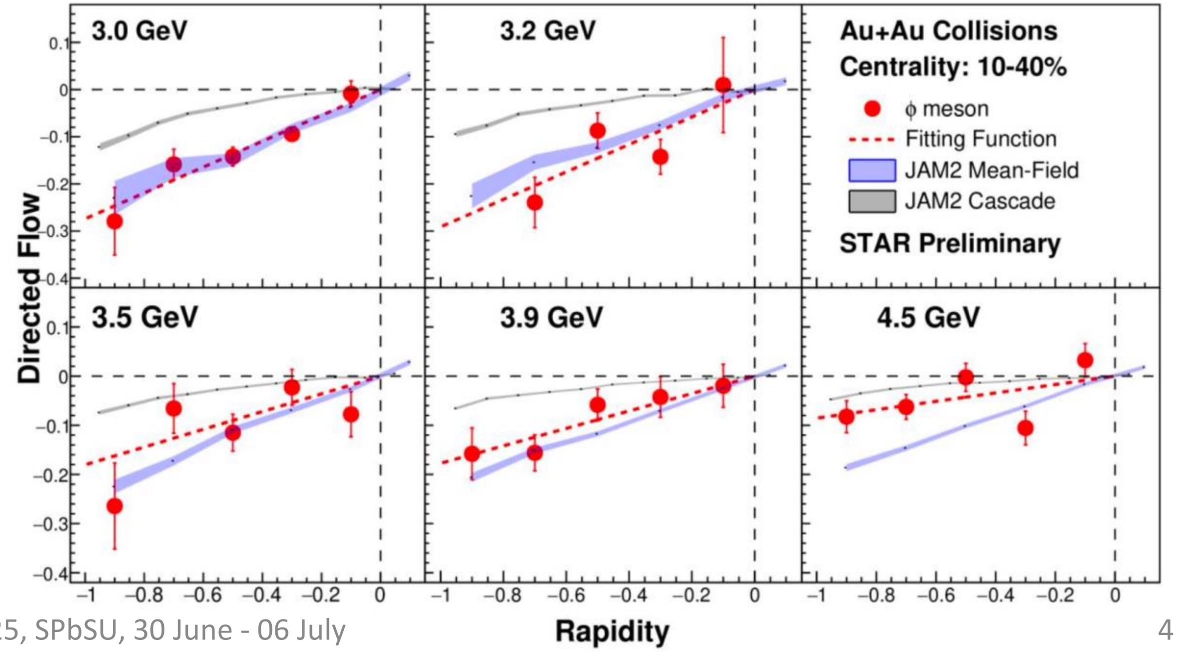

Directed flow of light nuclei

Monotonic energy dependence for all particles, deuteron has the opposite sign compared to protons

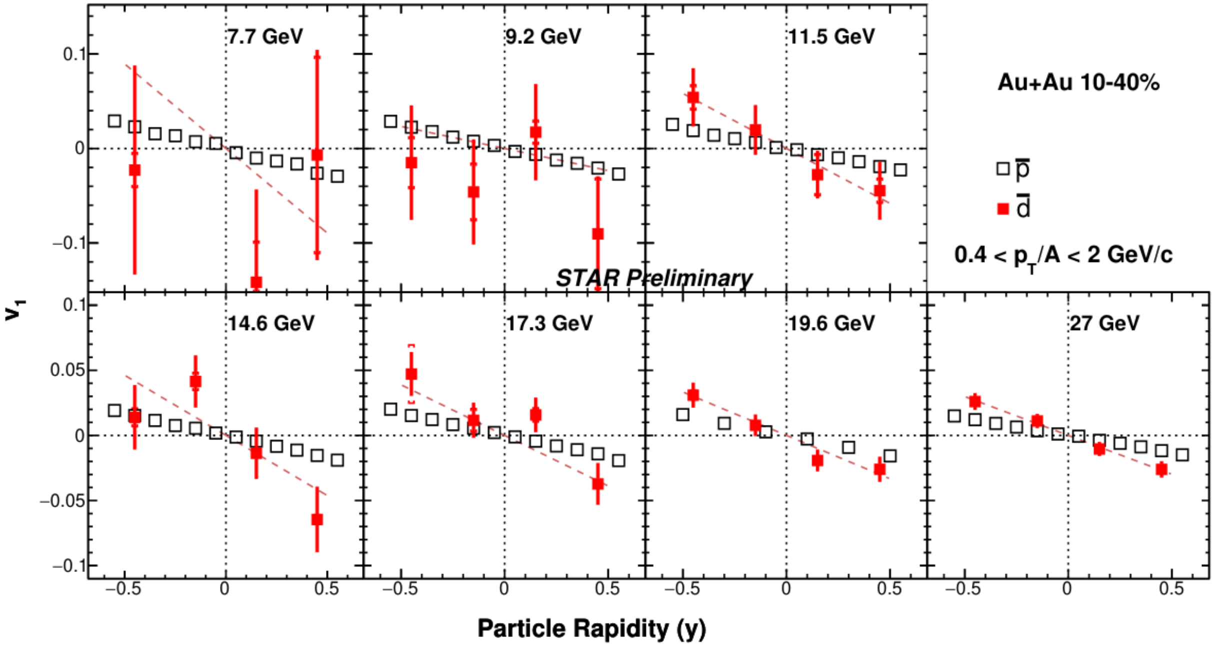

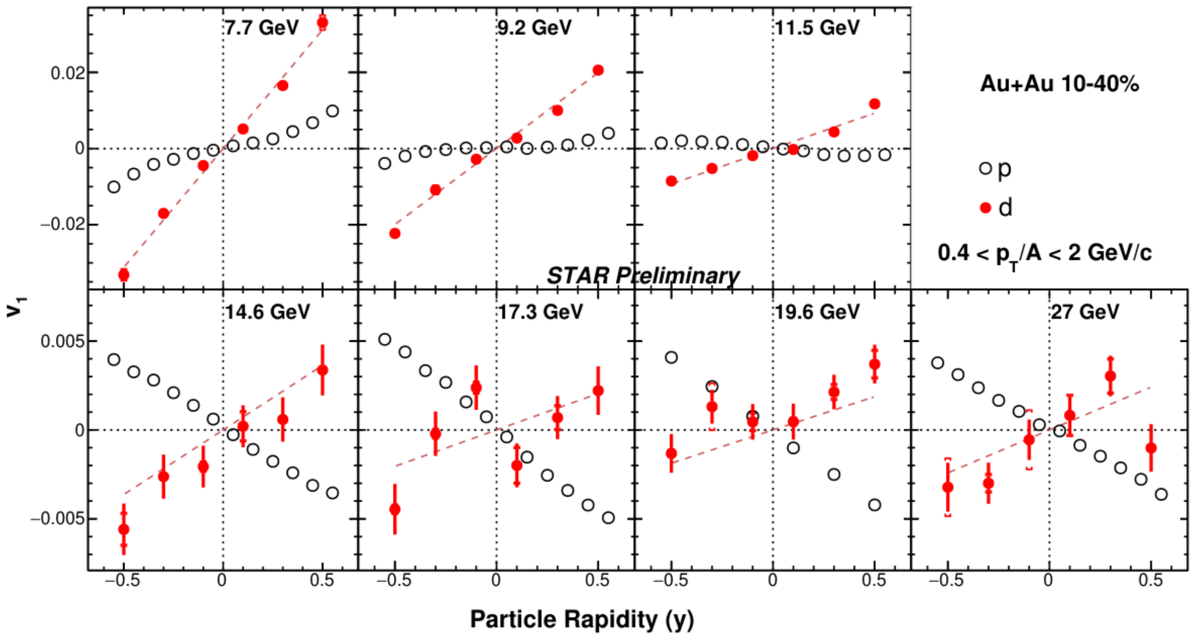

Different production mechanism for deuterons, additional in-medium effects?
Theoretical input is needed to describe the antiflow of deuterons

Energy dependence of the v_2 NCQ-scaling

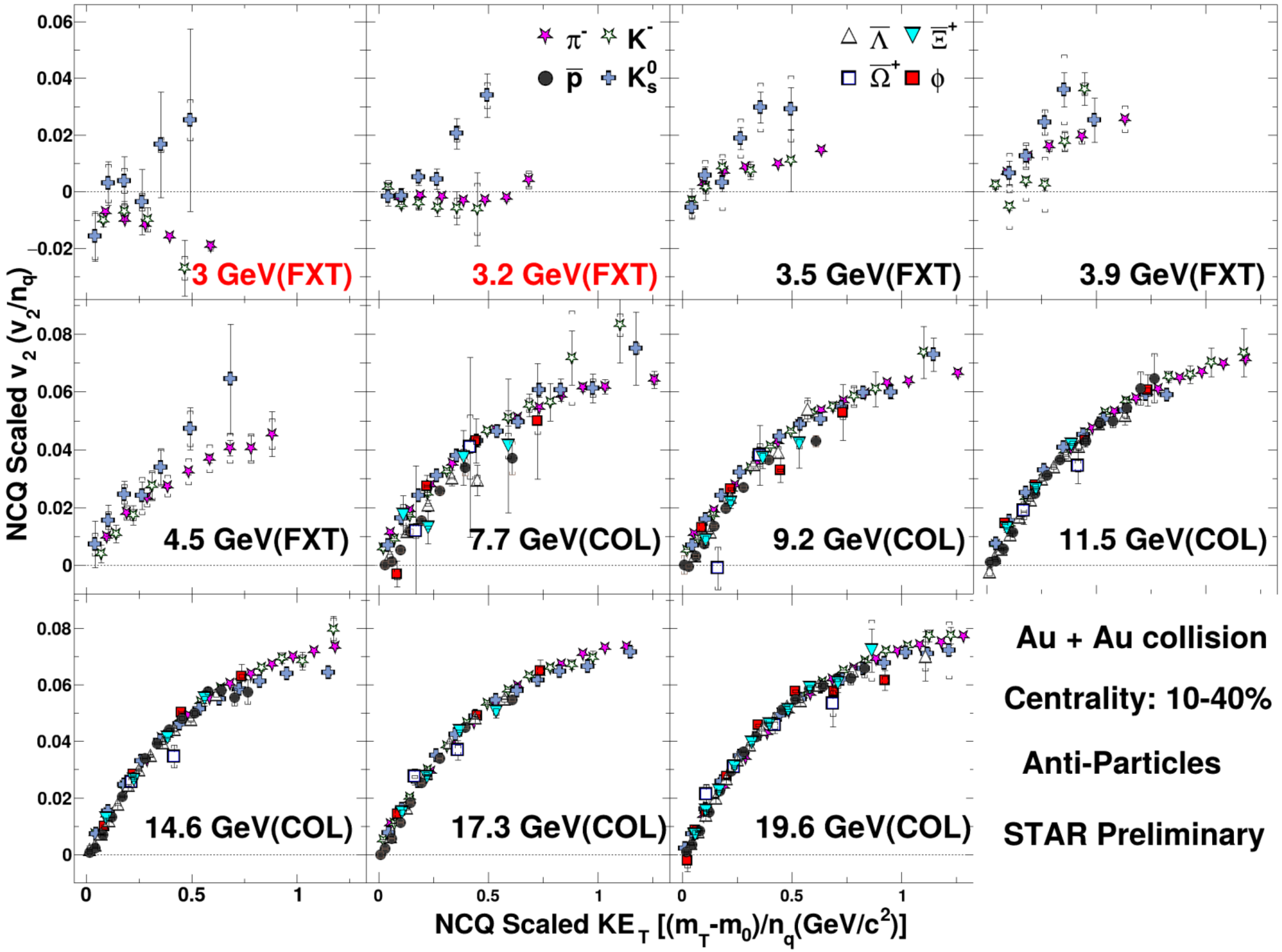

The number of constituent quarks scaling is completely broken at 3 and 3.2 GeV and gradually restores at higher energies.

Transition from pure hadronic to partonic interactions with the increase of the collision energy.

Energy dependence of the v_2 NCQ-scaling

particles

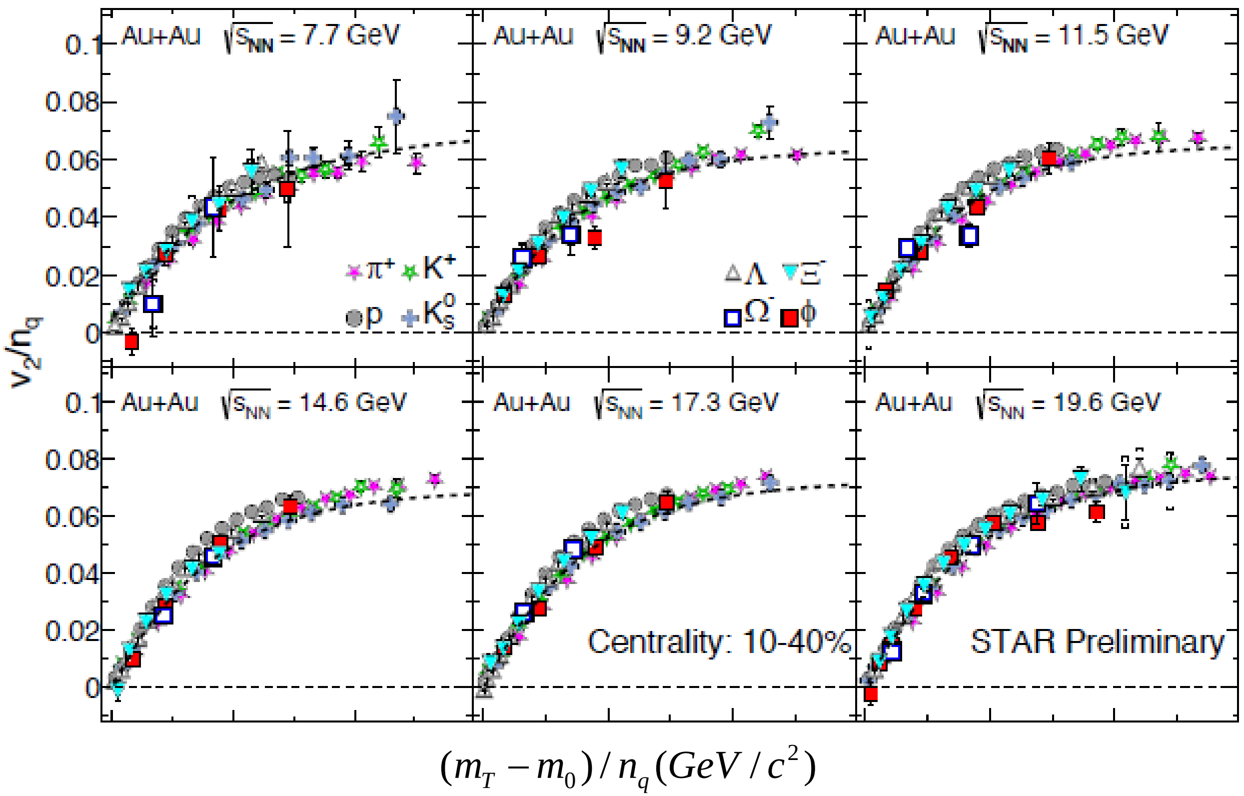

antiparticles

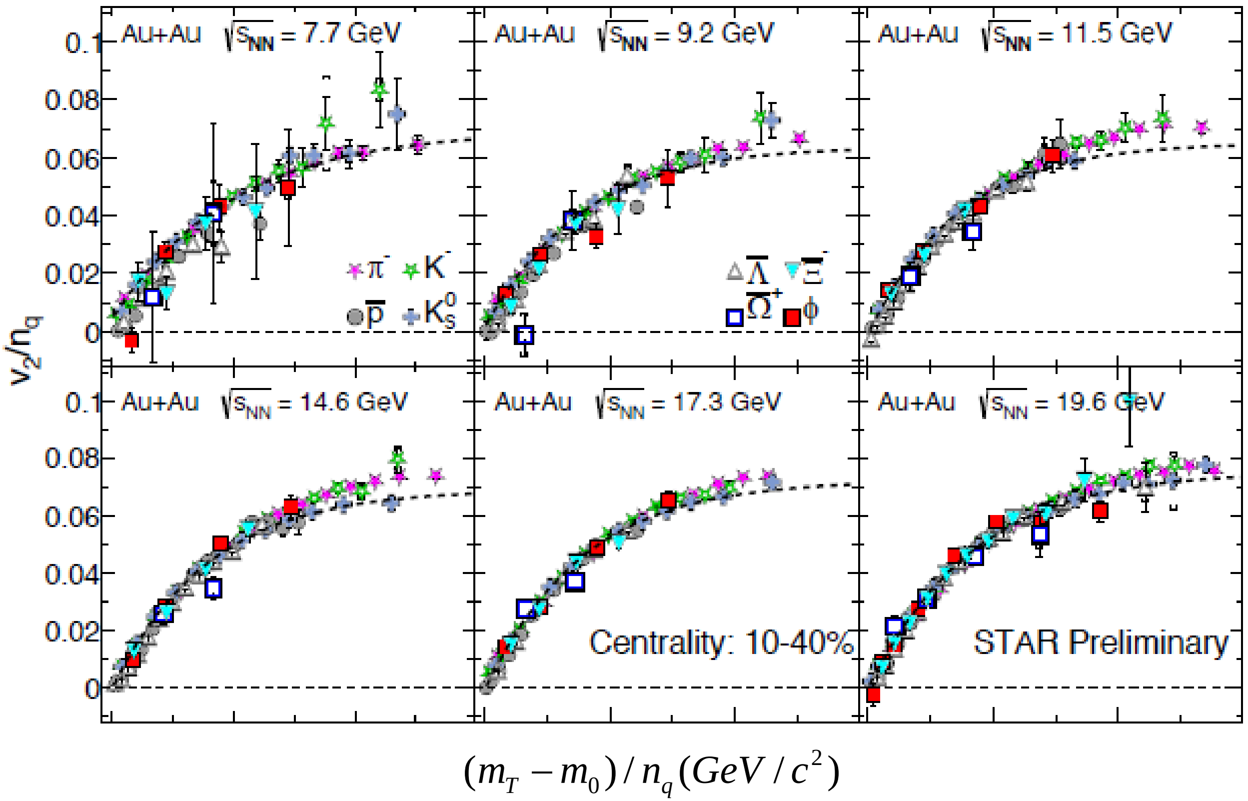

With better statistics from BES-II more precise measurements of **Ω** and **φ** mesons were done
All particles follow NCQ-scaling at this energies

Correlation femtoscopy

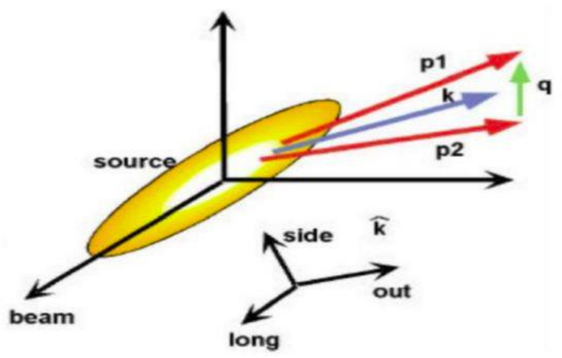

Two particle femtoscopy provides information on possible interactions and bound states in different systems

Correlation function can be affected by Quantum Statistics (QS), Final State Interaction (FSI), Coulomb Effect (CE)

$$C(k^*) = \frac{P(\vec{p}_a, \vec{p}_b)}{P(\vec{p}_a) \cdot P(\vec{p}_b)} = \int d^3r^* S(r^*) \left|\Psi(r^*, k^*)\right|^2 = \mathcal{N} \frac{N_{same}(k^*)}{N_{mixed}(k^*)}$$

statistical — theoretical — experimental

$$C(k^*) \begin{cases} > 1 & \text{attraction} \\ = 1 & \text{no correlation} \\ < 1 & \text{repulsion} \end{cases}$$

Third body effect at low energies

Difference in positive and negative charged pion CF can be described by the spectators charge

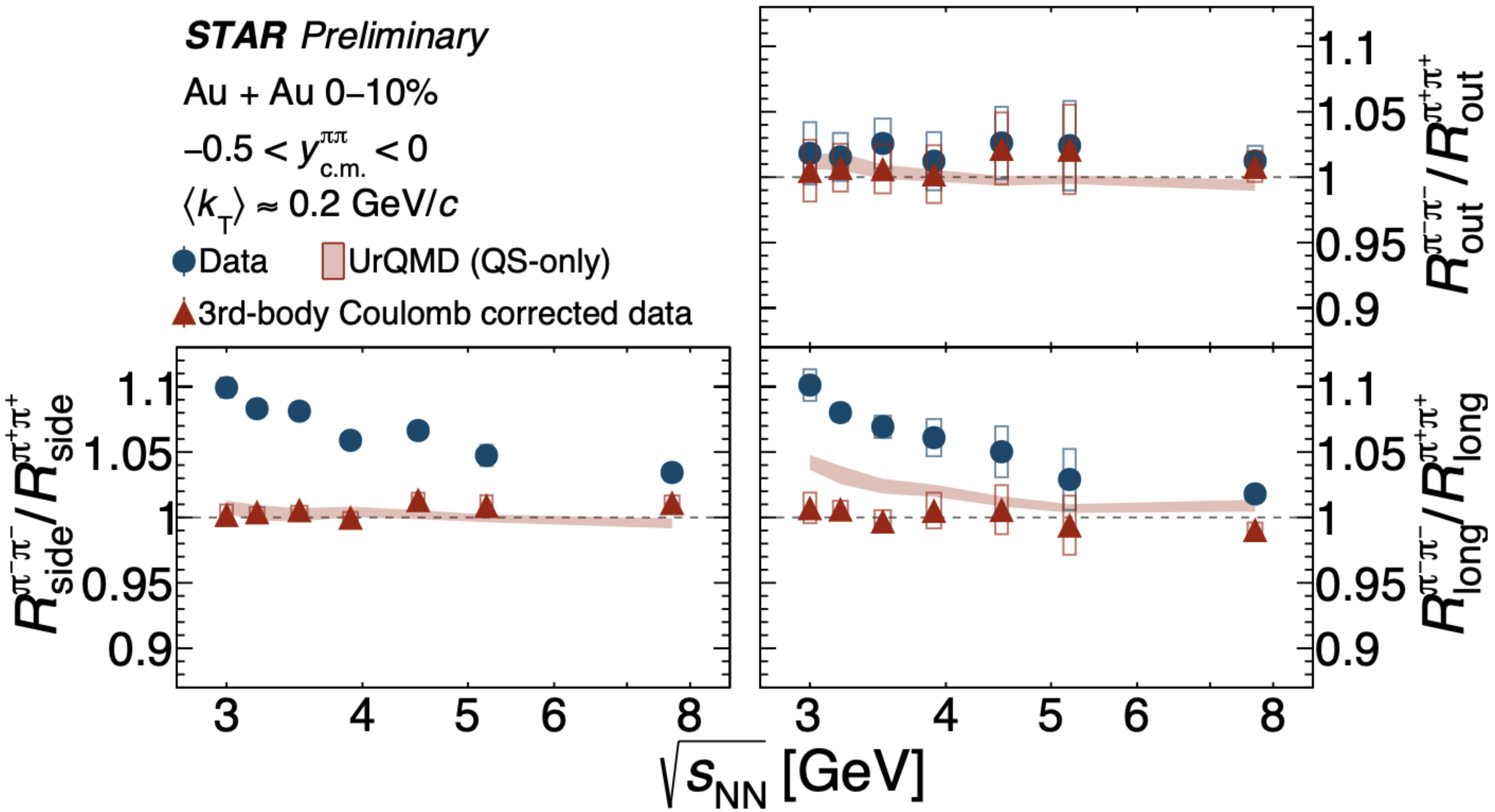

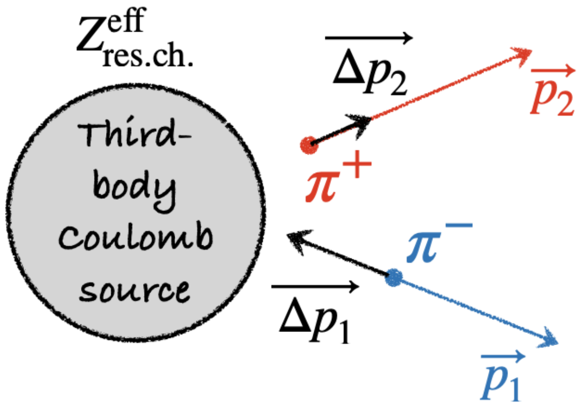

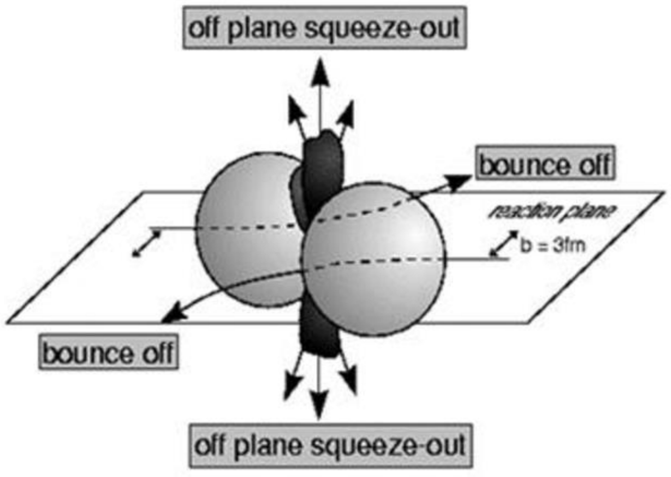

Λ-Λ correlation function

No indication of an attractive behavior in two-**Λ** system

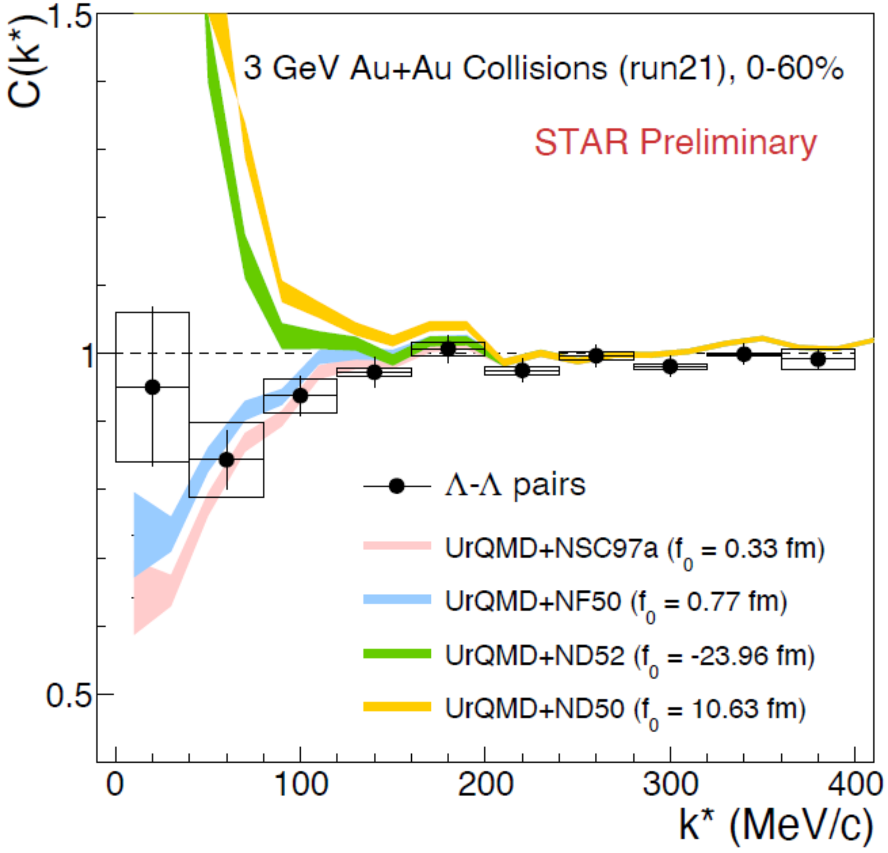

There are other possible exotic states especially in strange sector which can be tested with femtoscopy

Particle	Mass (MeV)	Quark composition	Decay mode
f_0	980	$q\bar{q}s\bar{s}$	$\pi\pi$
a_0	980	$q\bar{q}s\bar{s}$	$\pi\eta$
K(1460)	1460	$q\bar{q}q\bar{s}$	$K\pi\pi$
$\Lambda(1405)$	1405	$qqqs\bar{q}$	$\pi\Sigma$
$\Theta^+(1530)$	1530	$qqqq\bar{s}$	KN
H	2245	uuddss	$\Lambda\Lambda$
$N\Omega$	2573	qqqsss	$\Lambda\Xi$
$\Xi\Xi$	2627	qqssss	$\Lambda\Xi$
$\Omega\Omega$	3228	ssssss	$\Lambda K^- + \Lambda K^-$

Strange particles production near the threshold

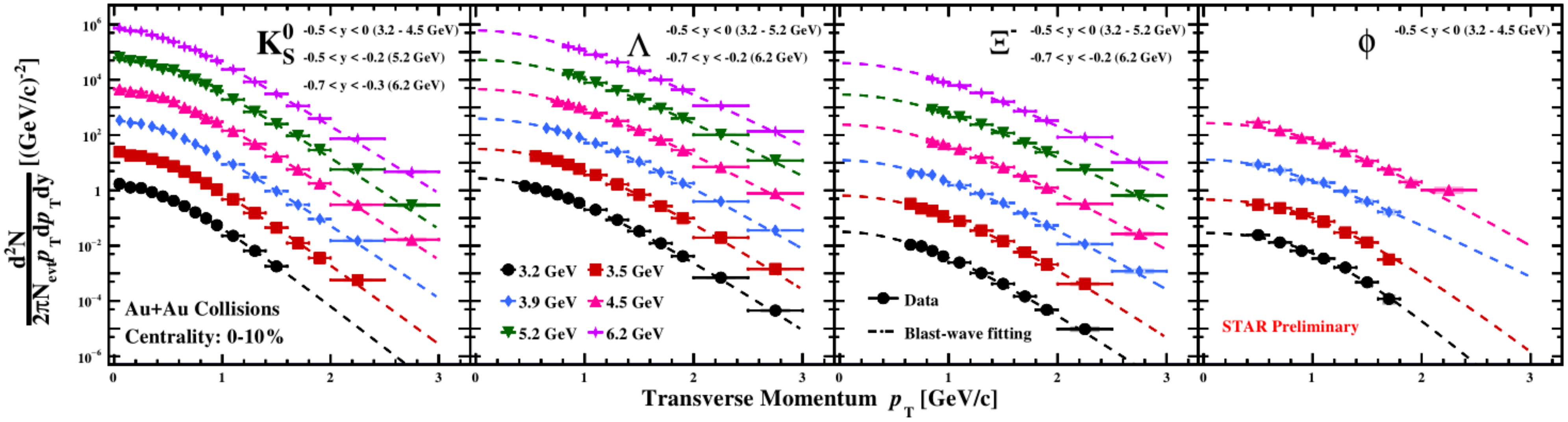

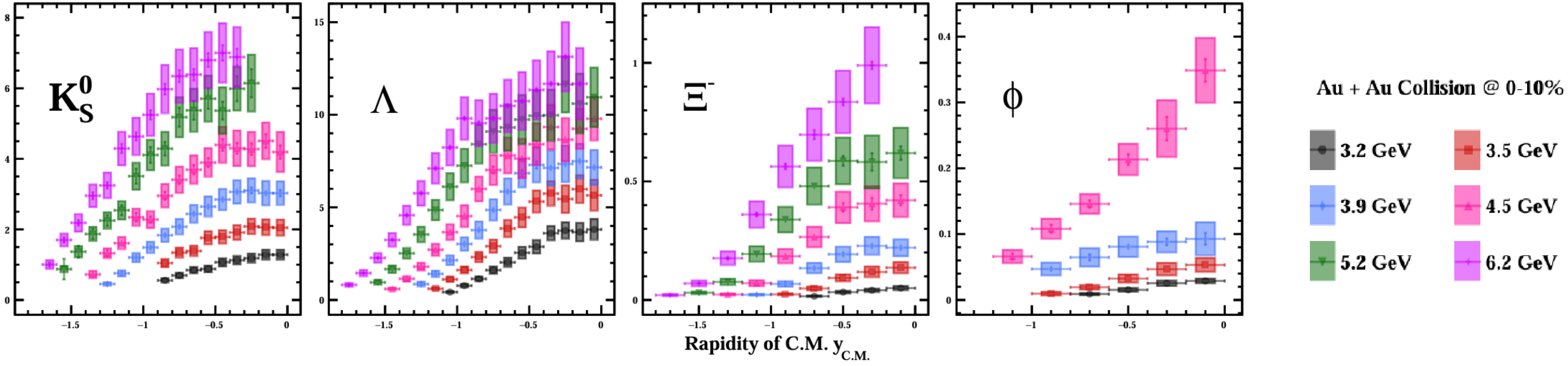

Strange particles production near the threshold

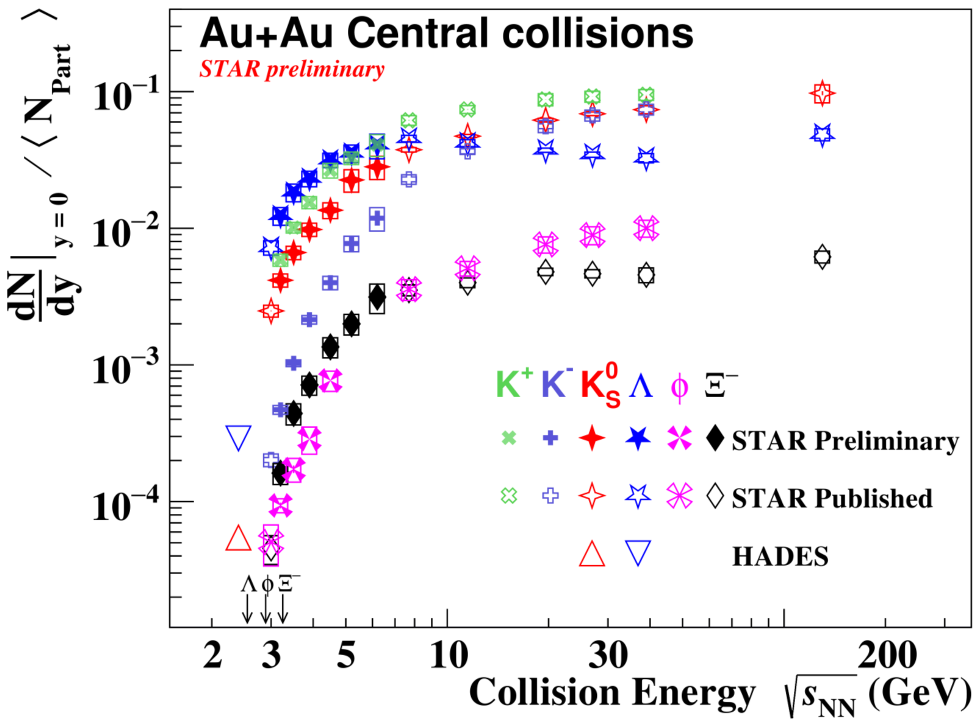

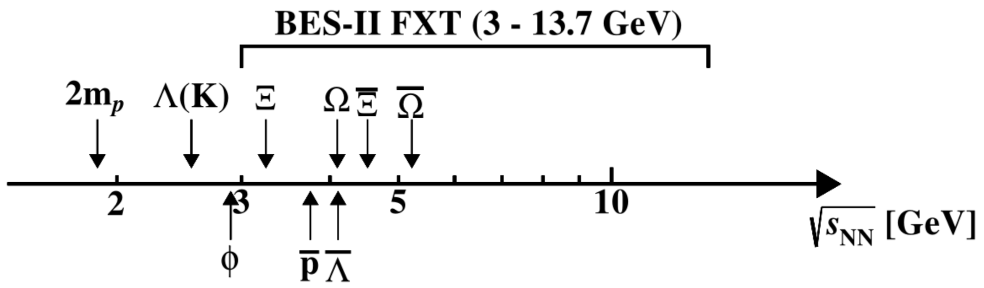

Rich structure in strangeness excitation functions

➢ Production mechanisms are different at low and high energies (high and low baryon density)

Partonic interaction (pair production)
gg → ss or **qq → ss**
Hadronic interaction (associated production)
BB → BYK or **BB → BΞKK**
B: N, p, **Δ**, etc. Y: **Λ**, **Σ**, etc. K: **K+**, **K0**

➢ Baryon-dominated to meson-dominated transitions
Ks0 and **Λ** mid-rapidity yield cross at ~ 8 GeV

➢ First measurement of **Ξ−** near- / sub-threshold energies in Au+Au collision

STAR Collab Phys. Rev. C 102, 034909 (2020);
Phys. Rev. C 110, 054911 (2024);
JHEP 2024, 139 (2024)
V. Vovchenko, et.al. Phys. Rev. C 93, 064906 (2016)
S. Wheaton, et.al. Comput.Phys.Commun.180(2009)

Strange particle ratios

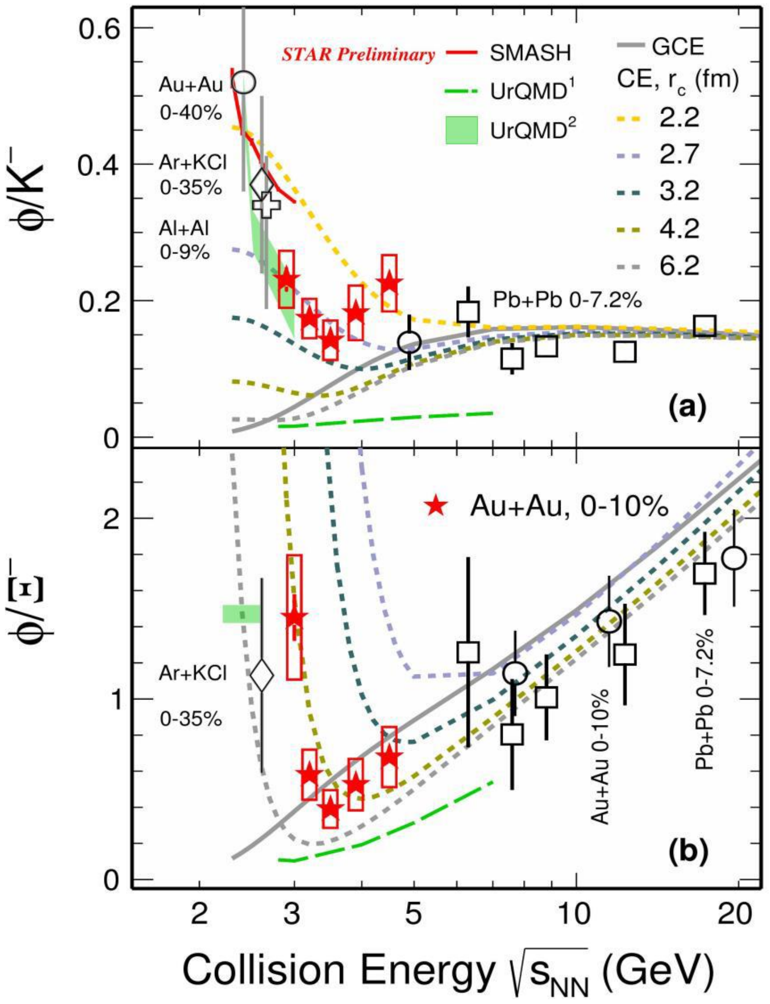

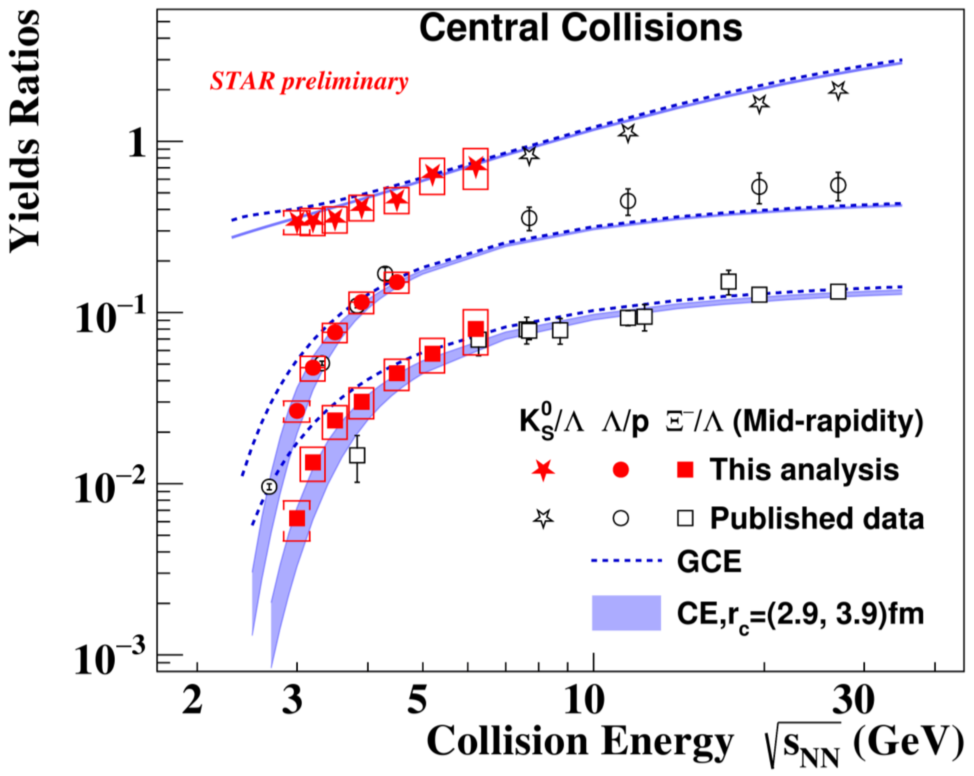

CE describe yield ratios with $r_c \sim 3-4$ fm, GCE fails below $\sqrt{S_{NN}} \sim 5$ GeV

Test of the medium properties in high baryon density region

STAR Collab. Phys. Lett. B 831, 137152 (2022)
UrQMD: Prog. Part. Nucl. Phys. 41 (1998) 225-370
UrQMD: J. Phys. G: Nucl. Part. Phys. 43 015104

Light nuclei production at FXT energies

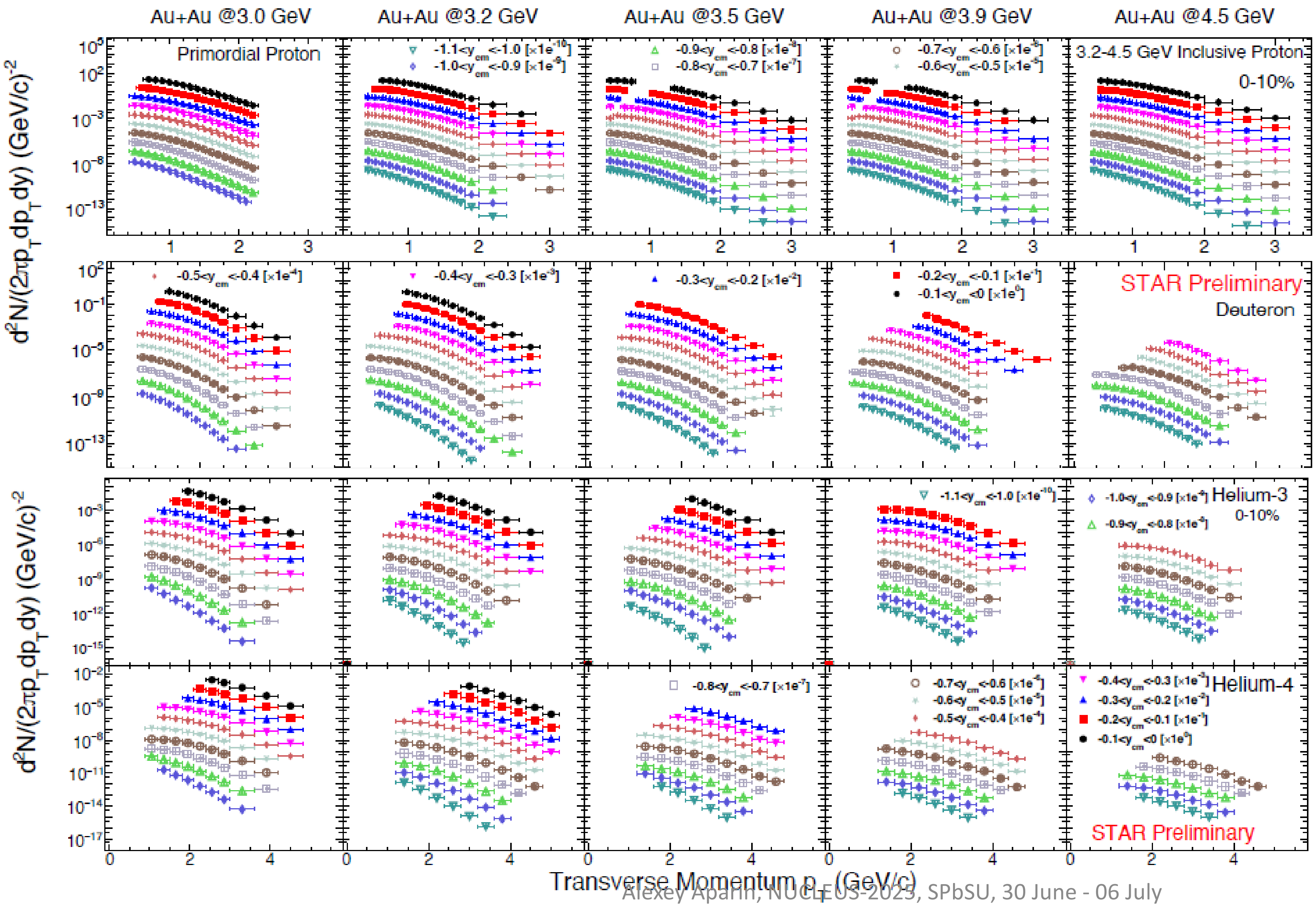

Light nuclei production

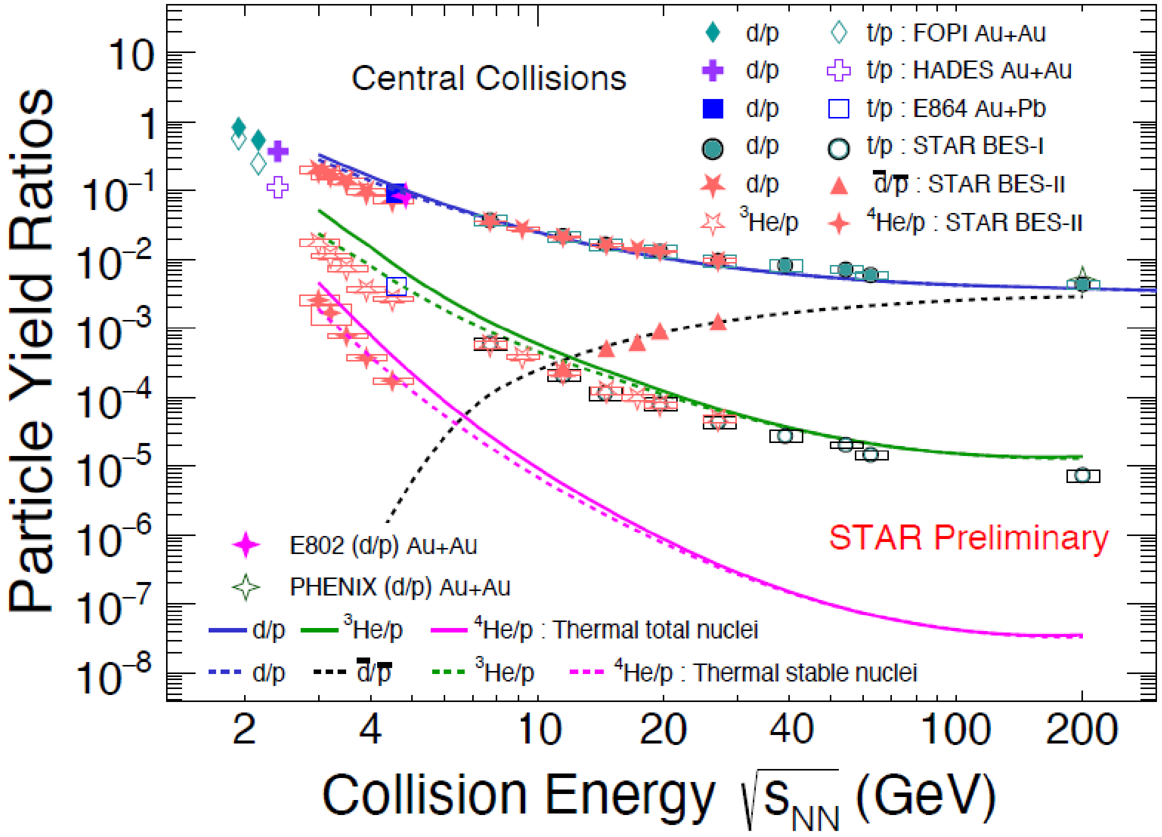

Clear energy dependence is observed for ratios of all particle types

The trends of ratios can be described qualitatively by the thermal model

He/p is overestimated by thermal model, possibly due to the hadronic re-scattering effect

Considering only stable nuclei, *He/p* from thermal model is consistent with the experiment data

[STAR Collab] Phys. Rev. C 96, 044904 (2017); Phys.Rev.Lett. 130 (2023) 202301;
[E802 Collab] Phys.Rev.C 60 (1999) 064901;[E864 Collab] Phys.Rev.C 61 (2000) 064908;
[FOPI Collab] Nucl.Phys.A 848 (2010) 366-427;V. Vovchenko, et al. Phys. Rev. C 93(2016) 6, 064906;

Kinetic freeze-out temperature

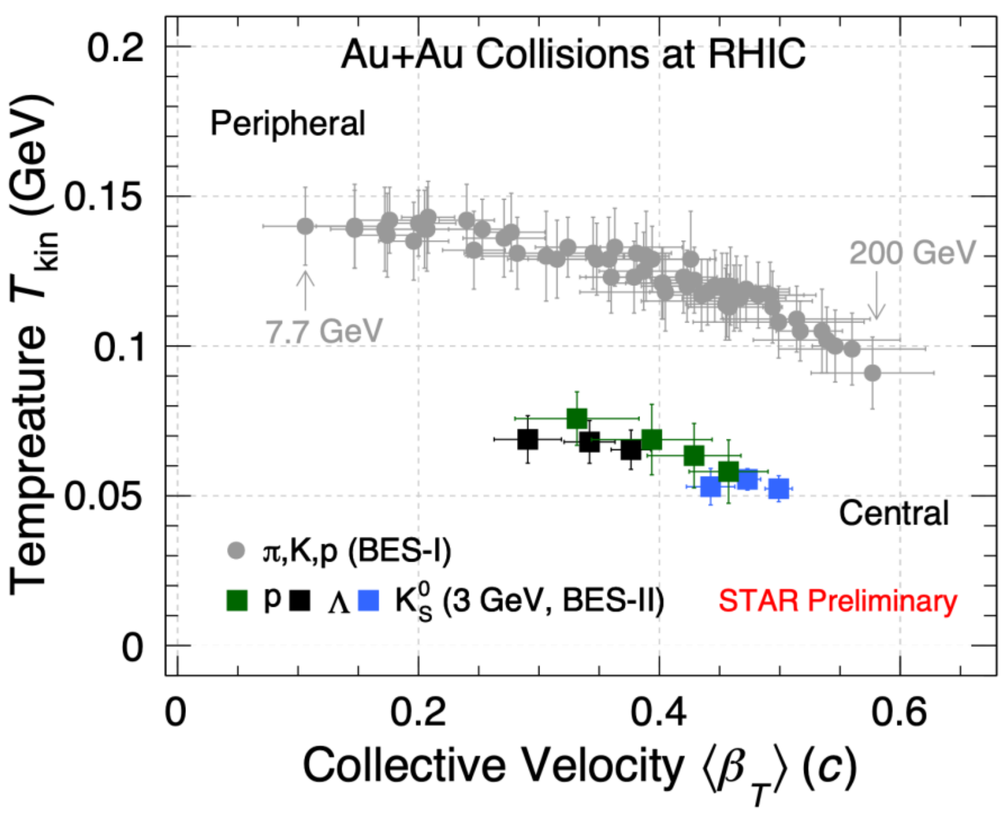

Change in medium properties (EOS) or expansion dynamics

Kinetic freeze-out temperature

A variety of experimental results demonstrates similar features of kinetic freeze-out at low energies

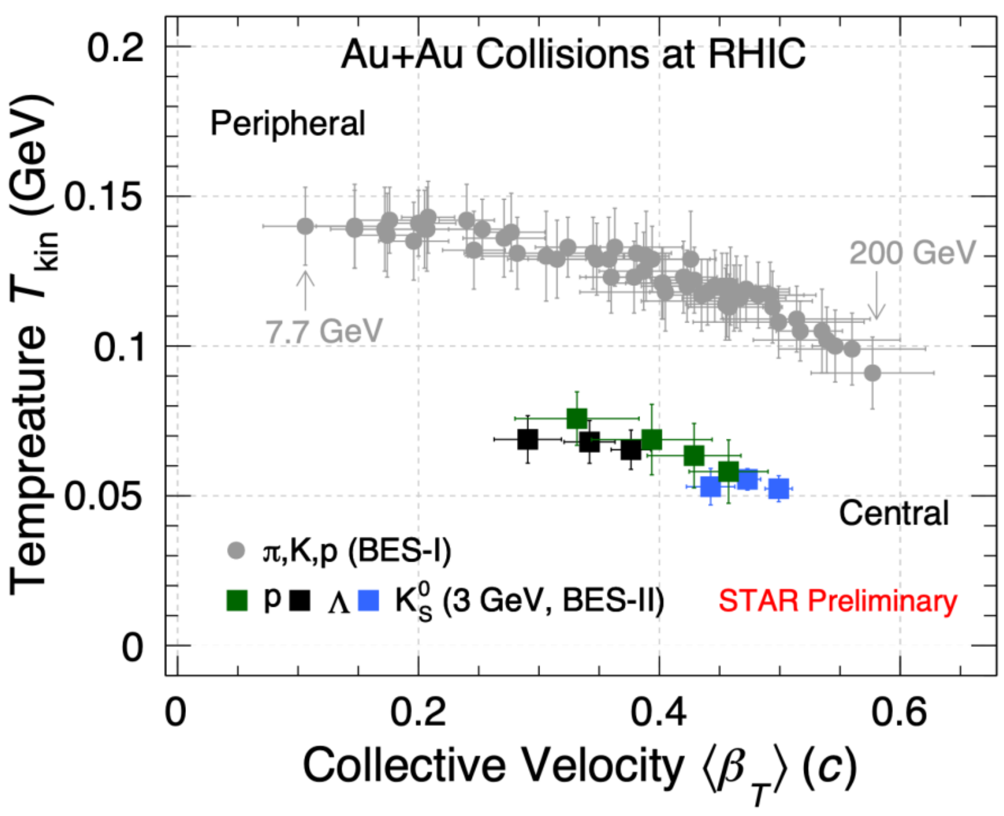

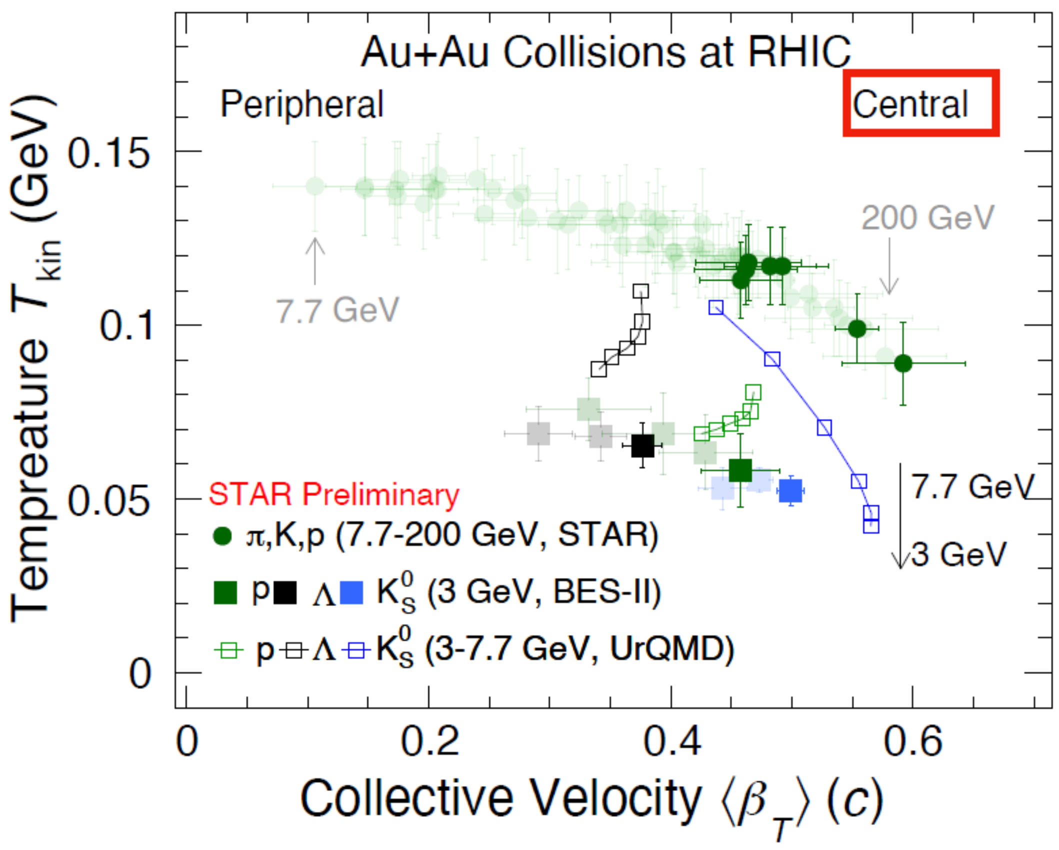

Change in medium properties (EOS) or expansion dynamics

STAR Collaboration. Phys. Rev. C 110, 054911 (2024); JHEP 2024, 139 (2024)

Kinetic freeze-out temperature

A variety of experimental results demonstrates similar features of kinetic freeze-out at low energies

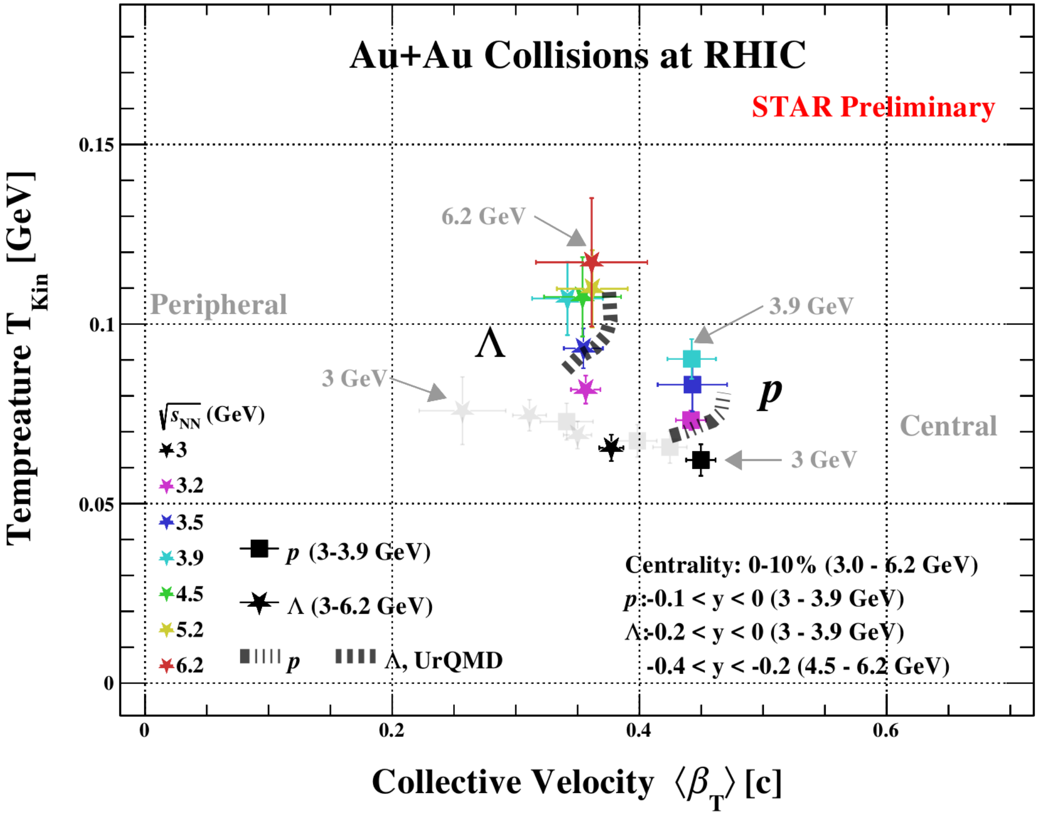

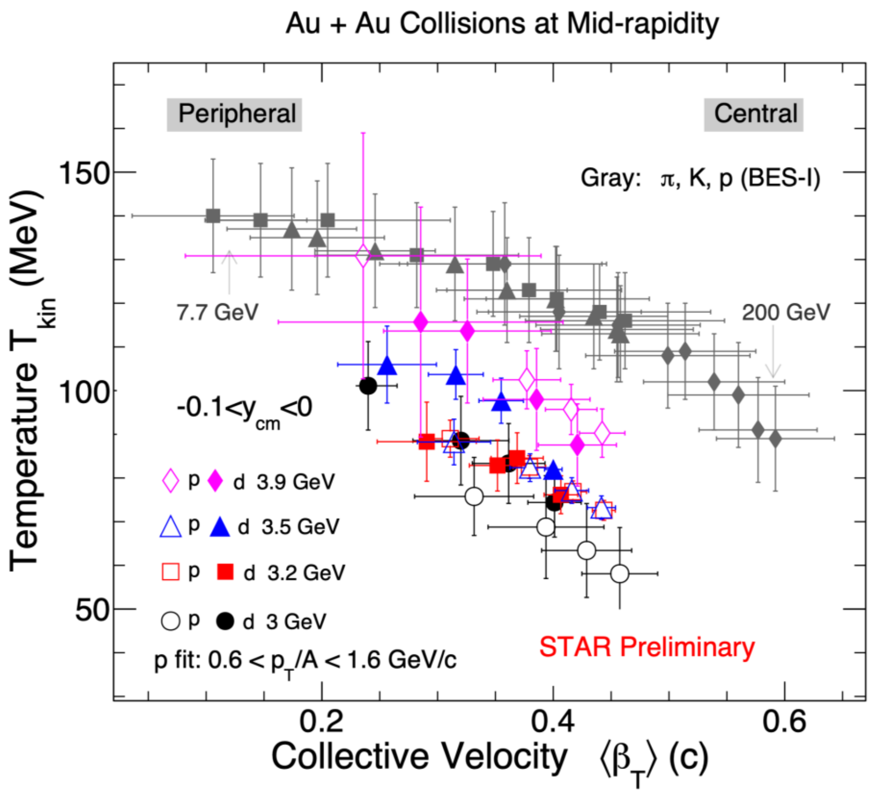

Gradual change in the temperature and radial velocity at FXT energies for mesons hadrons and light nuclei

STAR Collaboration. Phys. Rev. C 110, 054911 (2024); JHEP 2024, 139 (2024)

Production of hypernuclei

Interplay of two main processes at low energies:
- increasing baryon density
- strangeness canonical suppression

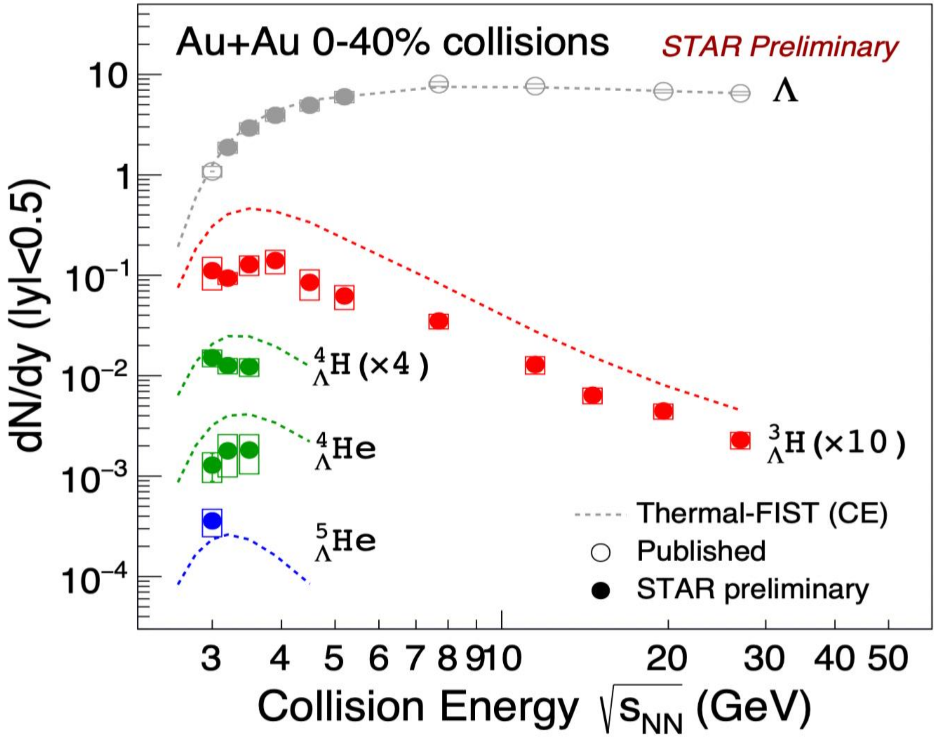

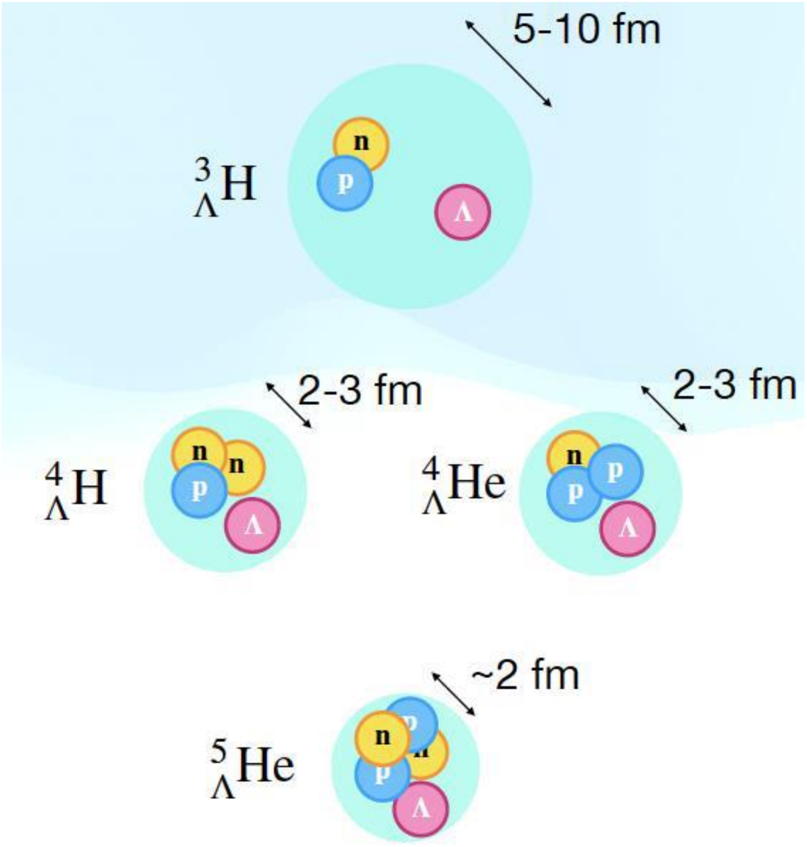

Thermal model describes hadron yields well, but not the hypernuclei

STAR, PRL 128, 202301 (2022)
V. Vovchenko et al., PRC 93, 064906 (2016)

Mean transverse momentum of hypernuclei

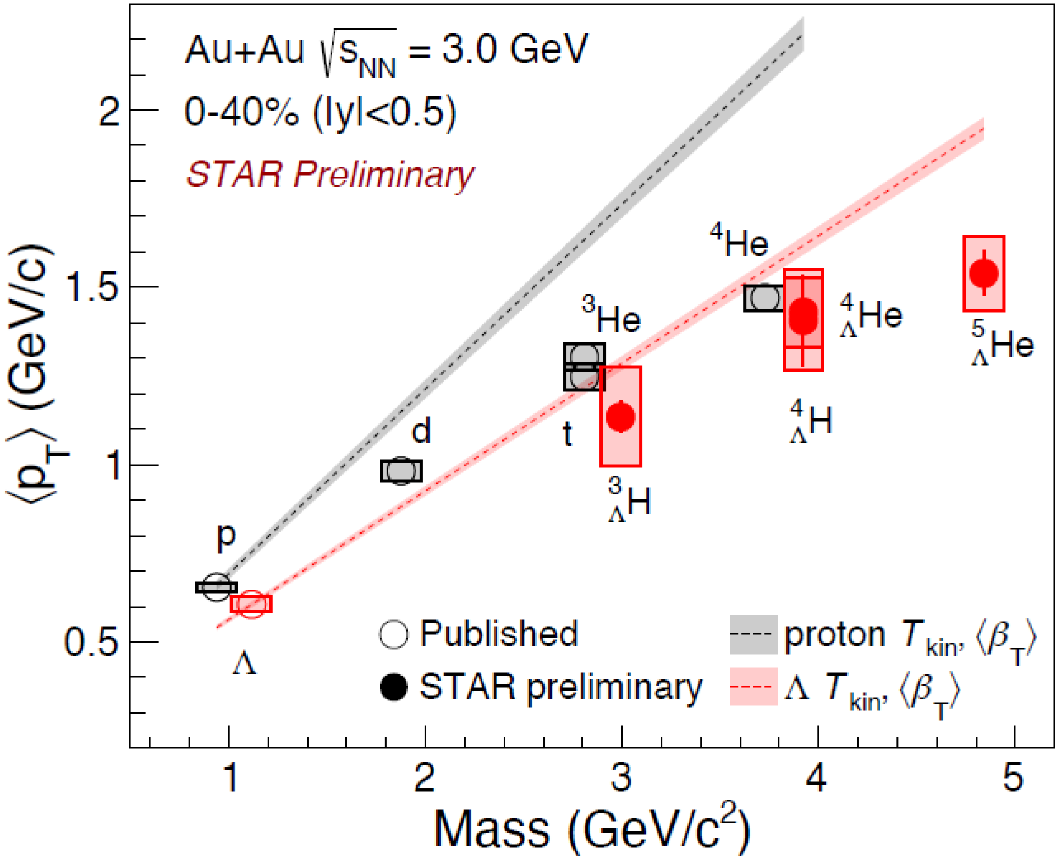

Thermal model calculations doesn't quantitatively describe the mass ordering of light and hypernuclei

Mean transverse momentum tends to be lower than hydrodynamic-inspired blastwave model expectation at high baryon density

Points to the coalescence production mechanism for light and hypernuclei

Net-proton cumulant measurements at FXT energies

Significant enhancement of cumulants above baseline for low moments

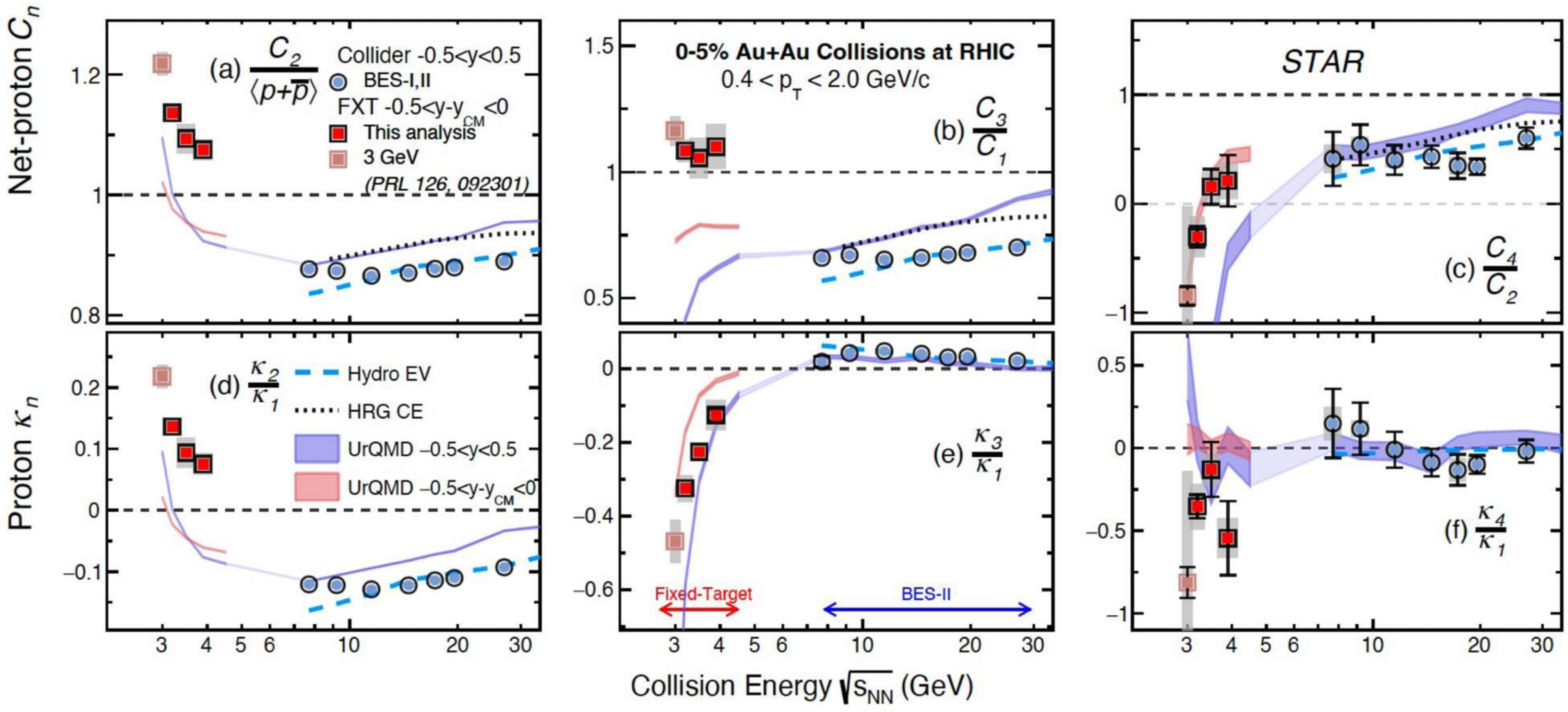

Significant deviations from non-critical baseline

Energy dependence of C_4/C_2

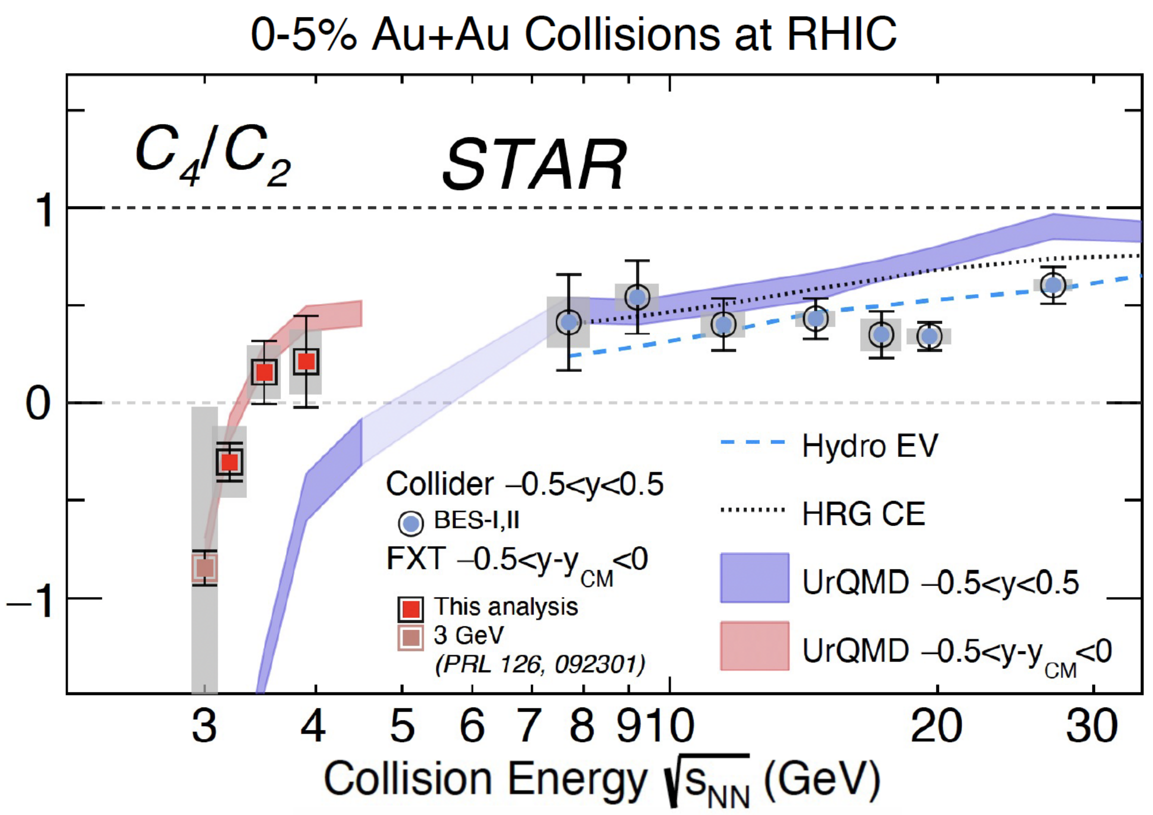

At FXT energies model calculations are consistent with the experimental results
At higher energies data points deviates from the model baseline

2 – 5 σ deviation from calculations without CP and peripheral data

The highest (lowest) significance level of 5σ (2σ) deviation corresponds to the case of peripheral collision data (hydro EV calculations) taken as the baseline.

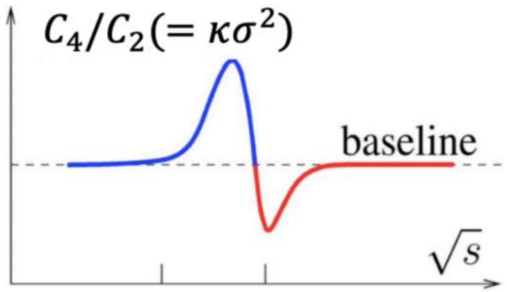

STAR Collab PRL 126, 092301
STAR: arXiv:2504.00817

Global polarization of Λ and anti-Λ

See report by Egor Alpatov
Sunday 13-50

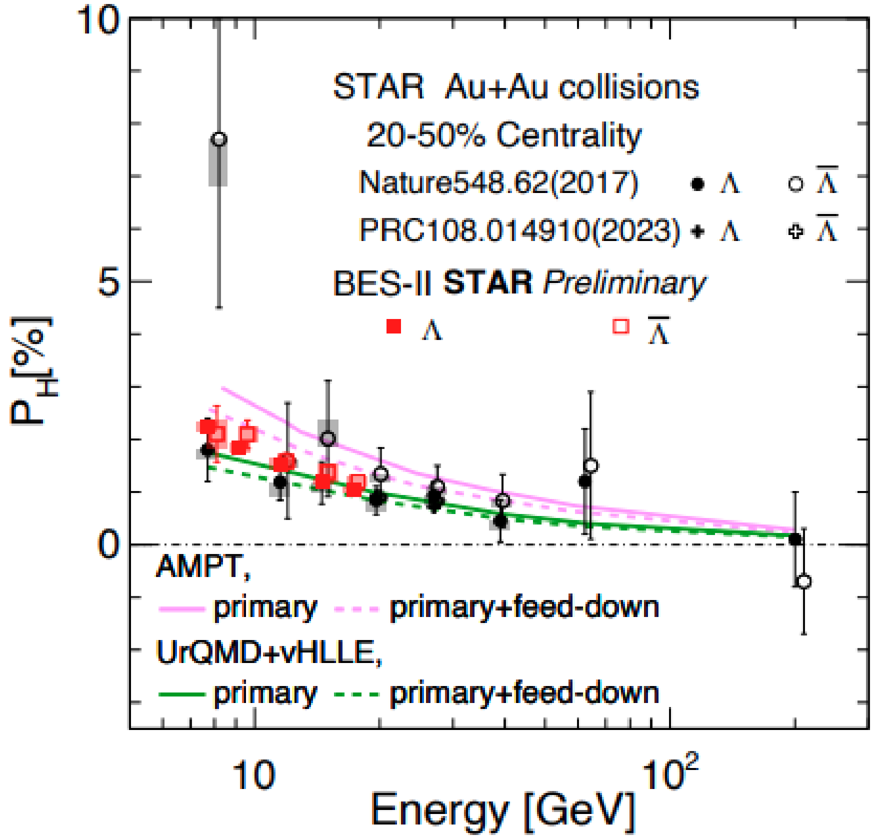

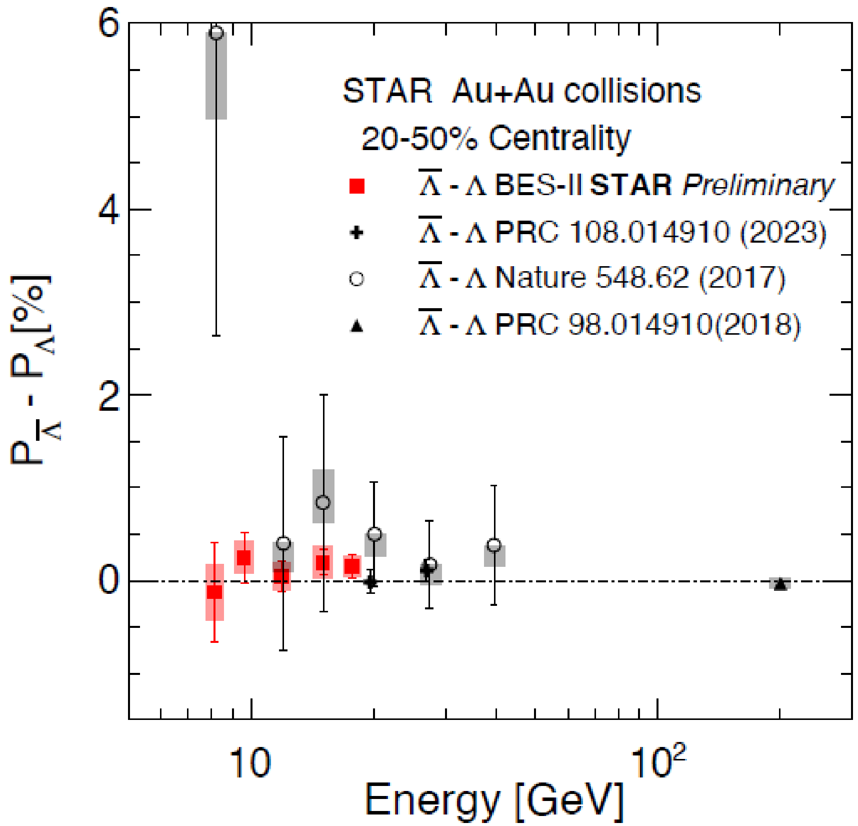

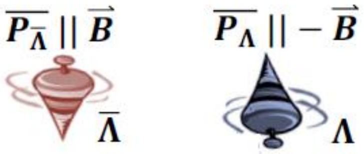

Upper limit on late-stage magnetic field $B \lesssim 10^{13}$ T (95% confidence level)
STAR, PRC 108, 014910 (2023)

Global polarization of Ξ and Ω

See report by Egor Alpatov
Sunday 13-50

Global polarization of Ξ and Ω follows the same trend which was previously established for Λ

Model calculation: H. Li, X. Xia et al Phys. Lett. B 827, 136971 (2022)

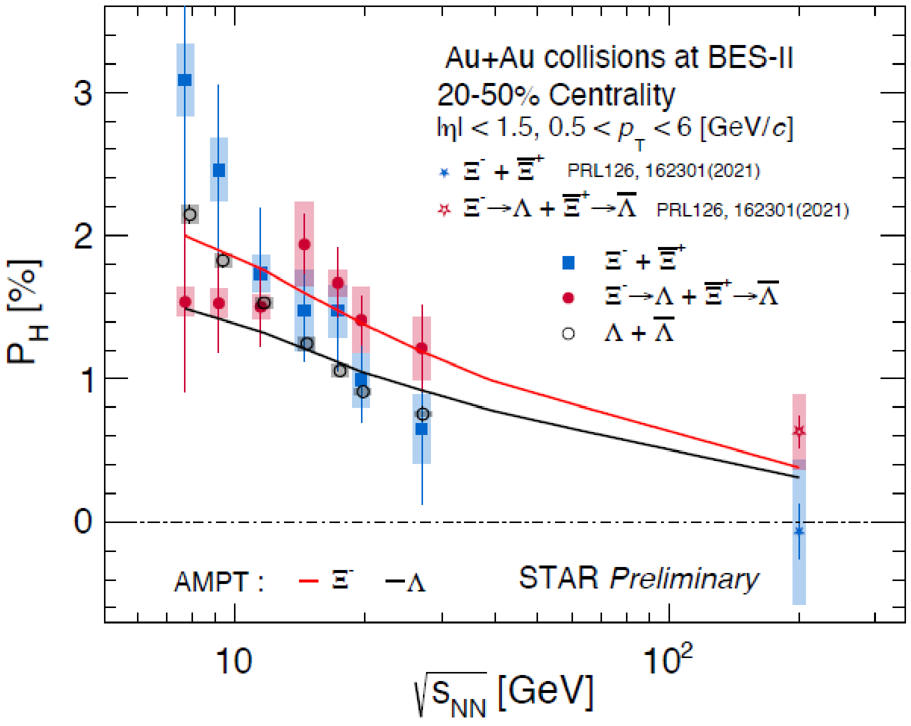

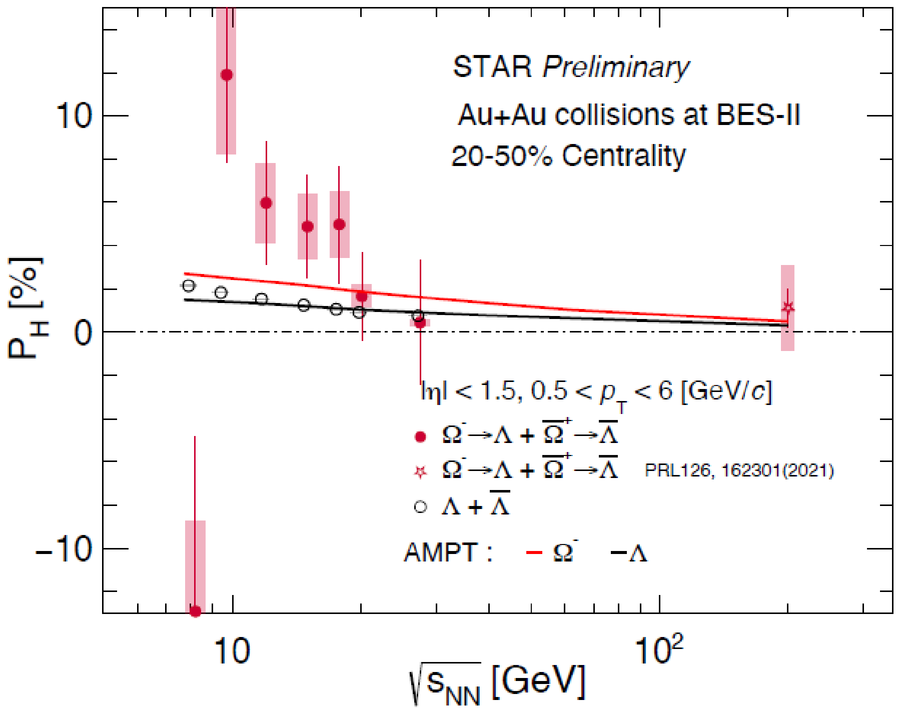

Possible **Λ, Ξ, Ω** global polarization difference from different s quark polarization?

$$P_\Lambda \sim P_\Xi \cong P_S \quad \text{assuming that} \quad P_{u,d} \sim P_S \qquad \text{and} \qquad P_\Omega \sim \frac{5}{3} P_\Lambda$$

Z.-T. Liang and X.-N. Wang, PRL 94, 102301 (2005)
Hui Li et al., PLB 827, 136971(2022)

Summary

STAR continues to report new data from the Beam Energy Scan at 7 collider and 13 fixed target energies in the energy range $\sqrt{s_{NN}}$ from 3 to 54.4 GeV where transition from hadronic to quark-gluon degrees of freedom is expected

Particle production at low collision energies demonstrates change in the kinetic freeze-out temperature and radial velocity extracted from meson, baryon and light nuclei

Breaking of the NCQ-scaling of elliptic flow is observed below 3.2 GeV and gets gradually restored with the increase in collision energy

New precise measurements of the net-proton cumulant ratios has demonstrated deviation from model calculations without critical point and peripheral data at 19.6 GeV at 2 – 5 σ level

Precise measurements of Λ global polarization showed no significant difference between particles and antiparticles

Global polarization of Ξ and Ω follows the same trend which was previously established for Λ

Thank you for the attention!

STAR 25 YEARS

STAR detector

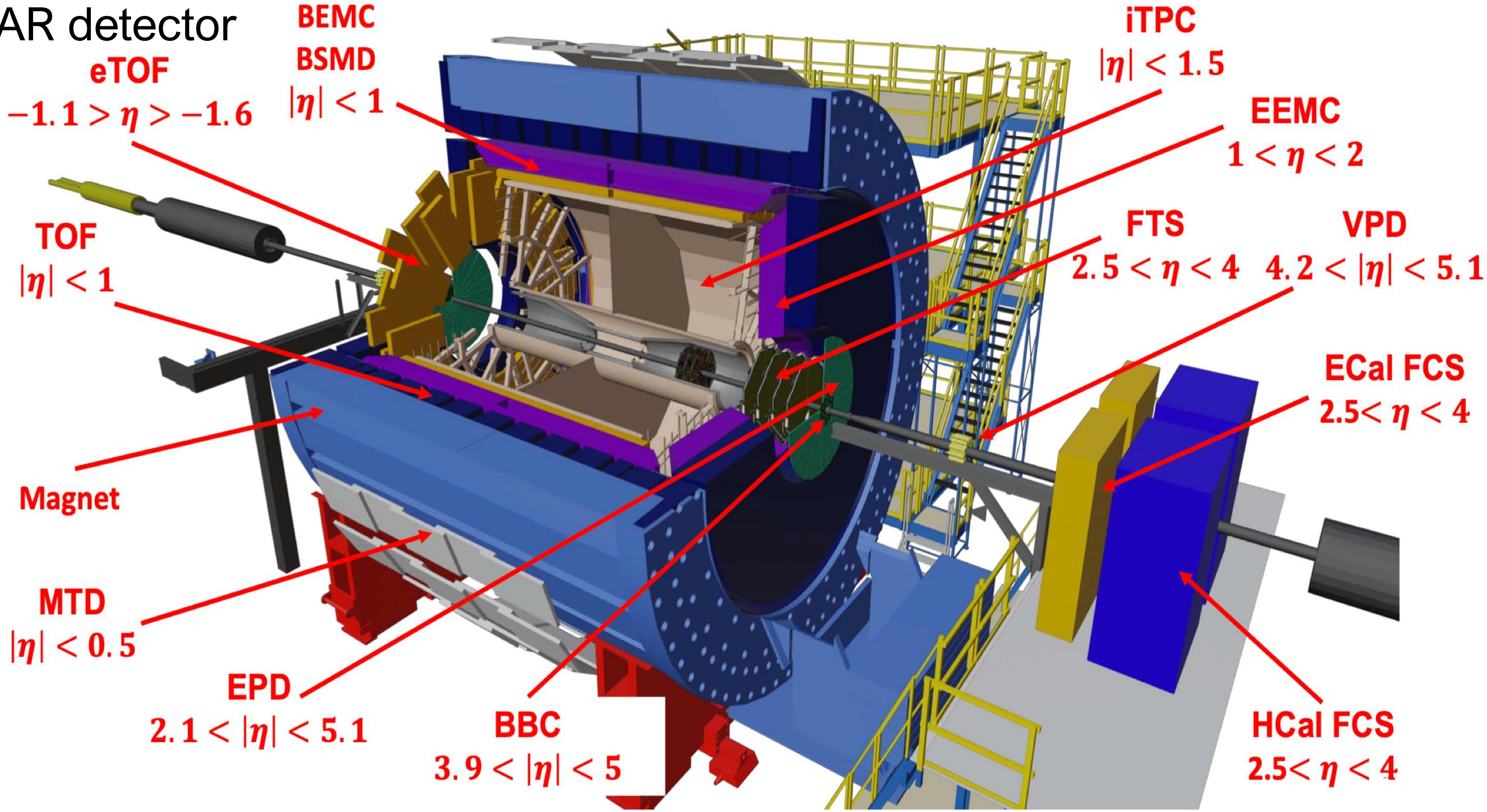

Extended rapidity coverage with the recent upgrades
Improved detector plane resolution
Improved particle identification capabilities

Directed flow of light nuclei

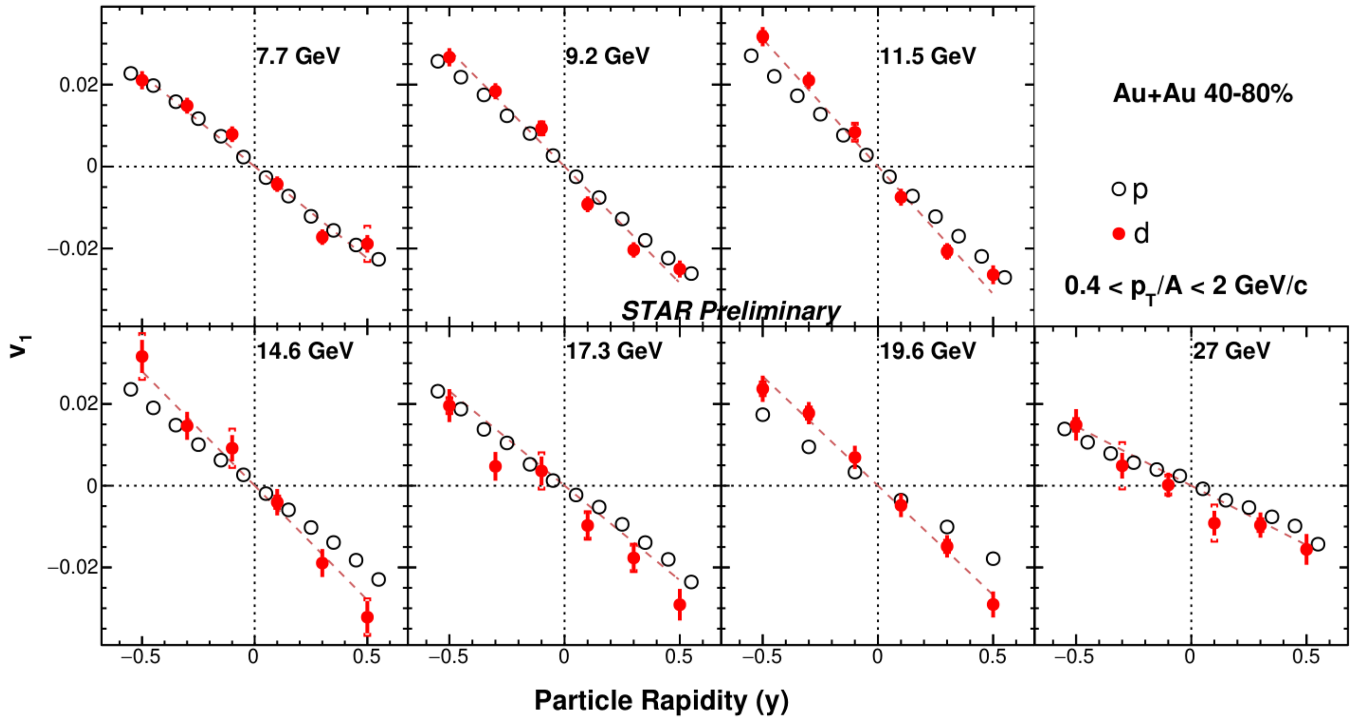

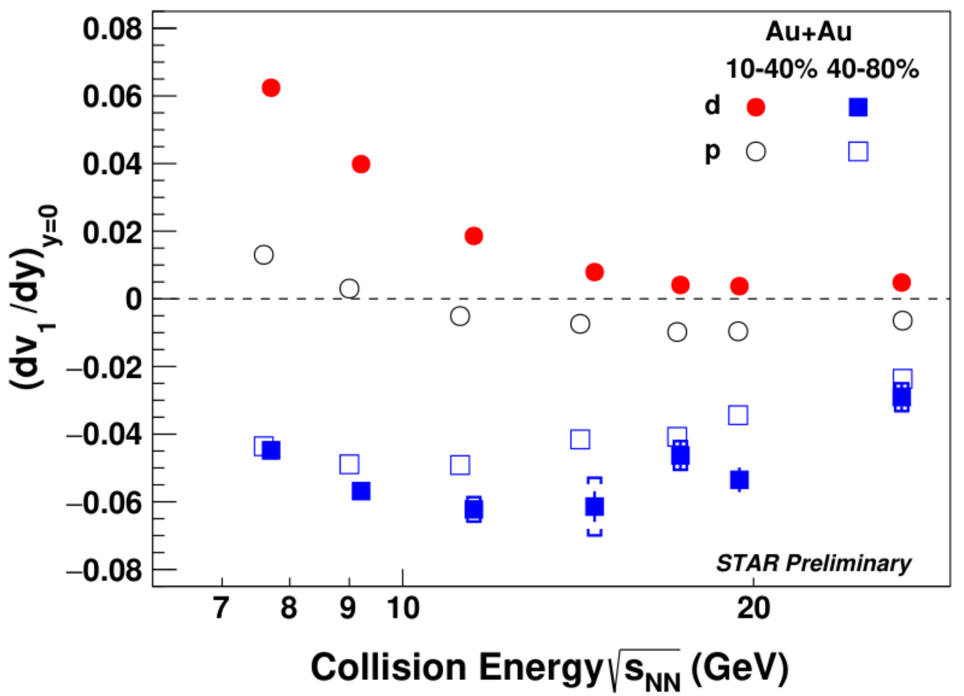

Same v1 sign but no A scaling, dv1/dy sign changes from mid-central to peripheral collisions

Net-proton cumulant measurements at collider energies